Intrinsic Barriers for Electron and Hydrogen Atom Transfer Reactions of Biomimetic Iron Complexes

Justine P. Roth, Scott Lovell,[†] and James M. Mayer*

Contribution from the Department of Chemistry, Box 351700, University of Washington, Seattle, Washington 98195-1700

Received November 29, 1999

Abstract: Self-exchange reactions between high-spin iron complexes of 2,2′-bi-imidazoline (H$_2$bim) have been investigated by the dynamic NMR line-broadening technique. Addition of the ferric complex [Fe^{III}(H$_2$bim)$_3$]$^{3+}$ causes broadening of the ^{1}H NMR resonances of the ferrous analogue, [Fe^{II}(H$_2$bim)$_3$]$^{2+}$. This indicates electron self-exchange with $k_{e^-} = (1.7 \pm 0.2) \times 10^4$ M^{-1} s^{-1} at 298 K in MeCN-d_3 ($\mu = 0.1$ M). Similar broadening is observed when the deprotonated ferric complex [Fe^{III}(Hbim)(H$_2$bim)$_2$]$^{2+}$ is added to [Fe^{II}(H$_2$bim)$_3$]$^{2+}$. Because these reactants differ by a proton and an electron, this is a net hydrogen atom exchange reaction. Kinetic and thermodynamic results preclude stepwise mechanisms of sequential proton and then electron transfer, or electron and then proton transfer. Concomitant electron and proton (H$^{\bullet}$) transfer occurs with bimolecular rate constant $k_{H^{\bullet}} = (5.8 \pm 0.6) \times 10^3$ M^{-1} s^{-1}. This is a factor of 3 smaller than k_{e^-} under the same conditions. The H-atom exchange reaction exhibits a primary kinetic isotope effect $k_{NH}/k_{ND} = 2.3 \pm 0.3$ at 324 K, whereas no such effect is detected in the electron exchange reaction. Proton self-exchange between the two ferric complexes, [Fe^{III}(Hbim)(H$_2$bim)$_2$]$^{2+}$ and [Fe^{III}(H$_2$bim)$_3$]$^{3+}$, has also been investigated and is found to be faster than both the electron and H-atom transfer reactions. From kinetic analyses and the application of simple Marcus theory, an order of intrinsic reaction barriers $\lambda_{H^{\bullet}} > \lambda_{e^-} > \lambda_{H^+}$ is derived. The reorganization energies are discussed in terms of their inner-sphere and outer-sphere components.

Introduction

Hydrogen atom transfer reactions are attracting a resurgence of attention because of their importance in biological, synthetic, and industrial processes.[1] The relation of H$^{\bullet}$ transfer to proton-coupled electron transfer is of growing interest, especially in biochemical contexts.[2] Rates of H-atom transfer reactions have classically been understood using the Polanyi equation, which relates activation energy and enthalpic driving force (eq 1).[3]

$$E_a = \alpha(\Delta H) + \beta \tag{1}$$

Different classes of reactions are known to manifest different Polanyi parameters α and β. For example, oxygen radicals abstract H$^{\bullet}$ from substrates much faster than carbon radicals do at the same driving force. These differences are typically ascribed to polar effects, which in turn are often explained as different interactions of the radical's singly occupied orbital (its SOMO).[4] However, there are an increasing number of nonradical reagents, including transition metal complexes, that have been shown to mediate the net transfer of H$^{\bullet}$.[5] The reactivity of a number of the transition metal reagents correlate with the reactivity of oxygen radicals, following eq 1.[5b,6] These results are prompting a reexamination of the conventional ideas about radical reactivity.

The Marcus−Hush theory is a well-established model for outer-sphere electron-transfer reactions.[7] It is increasingly being used as a starting point for the understanding of other processes,[8] including dissociative electron transfer,[9] proton-coupled electron transfer,[2a−d] proton transfer,[10] atom transfer,[11] hydride transfer,[12]

† UW Chemistry staff crystallographer.

(1) See, for instance, (a) Stubbe, J. A.; van der Donk, W. A. *Chem. Rev.* **1998**, *98*, 705−762. (b) Meunier, B., Ed. *Biomimetic Oxidations Catalyzed by Transition Metal Complexes*; Imperial College Press, 2000. (c) Fossey, J.; Lefort, D.; Sorba, J. *Free Radicals in Organic Chemistry*; Wiley: 1995, New York. (d) Olah, G. A.; Molnár, Á. *Hydrocarbon Chemistry*; Wiley: New York, 1995. (e) Sheldon, R. A.; Kochi, J. K. *Metal Catalyzed Oxidation of Organic Compounds*; Academic Press: New York 1981.

(2) (a) Cukier, R. I.; Nocera, D. G. *Annu. Rev. Phys. Chem.* **1998**, *49*, 337−369. (b) Soudackov, A. V.; Hammes-Schiffer, S. *Chem. Phys. Lett.* **1999**, *299*, 503−510. (c) Binstead, R. A.; McGuire, M. E.; Dovletoglou, A.; Seok, W. K.; Roecker, L. E.; Meyer, T. J. *J. Am. Chem. Soc.* **1992**, *114*, 173−186. (d) Thorp, H. H. *Chemtracts: Inorg. Chem.* **1991**, *3*, 171−184. (e) Malström, B. G. *Acc. Chem. Res.* **1993**, *26*, 332. (f) Reference 16. (g) The importance of proton tunneling in enzyme catalysis is another aspect of this topic; see: Kohen, A.; Klinman, J. P. *Acc. Chem. Res.* **1998**, *31*, 397−404.

(3) (a) Kochi, J. K., Ed. *Free Radicals;* Wiley: New York 1973; Vol. 1, pp 275−331. (b) Tedder, J. M. *Angew. Chem., Int. ed. Eng.* **1982**, *21*, 401−410.

(4) Reference 1c, pp 52−55; 57ff.

(5) (a) Rüchardt, C.; Gerst, M.; Ebenhoch, J. *Angew. Chem., Int. Ed. Engl.* **1997**, *36*, 1406−1430. (b) Mayer, J. M. *Acc. Chem. Res.* **1998**, *31*, 441−450. (c) Gilbert, J.; Roecker, L. Meyer, T. J. *Inorg. Chem.* **1987**, *26*, 1126−1132. (d) Samsel, E. G.; Bullock, R. M. *J. Am. Chem. Soc.* **1990**, *112*, 6886−6898 and references therein.

(6) Roth, J. P.; Mayer, J. M. *Inorg. Chem.* **1999**, *38*, 2760−2761.

(7) (a) Marcus, R. A.; Sutin, N. *Biochim. Biophys. Acta* **1985**, *811*, 265−322. (b) Sutin, N. *Prog. Inorg. Chem.* **1983**, *30*, 441−499. (c) Marcus, R. A. *Angew. Chem., Int. Ed. Engl.* **1993**, *32*, 1111−1121. (d) Meyer, T. J.; Taube, H. In *Comprehensive Coordination Chemistry*; Wilkinson, G., Ed.; Pergamon: New York, 1987; Volume 1, Chapter 7.2, pp 331−384. (e) Eberson, L. *Electron Transfer Reactions in Organic Chemistry*; Springer: New York, 1987. (f) Wherland, S. *Coord. Chem. Rev.* **1993**, *123*, 169−199. (g) Barbara, P. F.; Meyer, T. J.; Ratner, M. A. *J. Phys. Chem.* **1996**, *100*, 13148−13168.

(8) (a) Marcus, R. A. *J. Phys. Chem.* **1968**, *72*, 891−899. (b) Cohen, A. O.; Marcus, R. A. *J. Phys. Chem.* **1968**, *72*, 4249−4256. (c) Babamov, V. K.; Marcus, R. A. *J. Chem. Phys.* **1981**, *74*, 1790. (d) Albery, W. J. *Annu. Rev. Phys. Chem.* **1980**, *31*, 227−263. (e) Murdoch, J. R. *J. Am. Chem. Soc.* **1983**, *105*, 2159−2164. (f) For a recent overview and extension: Guthrie, J. P. *J. Am. Chem. Soc.* **1998**, *120*, 1688−1694.
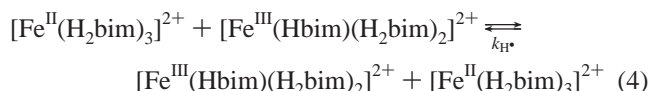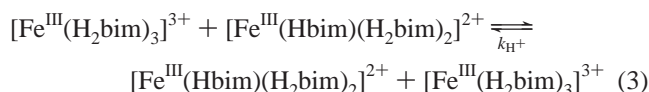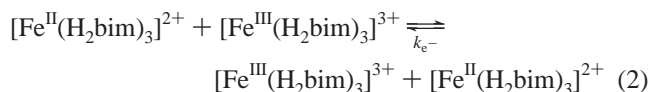
Chart 1
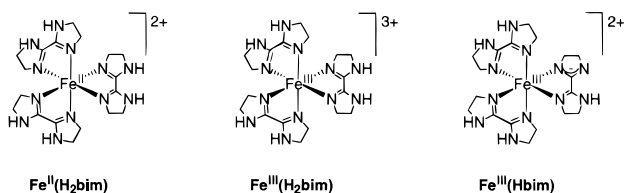
and others.[13] A key parameter in Marcus theory is the intrinsic barrier, $(1/4)\lambda$, defined as the kinetic barrier in the absence of driving force ($\Delta G = 0$). Marcus noted that the Polanyi (H•) and Brønsted (H+) equations are subsets of his theory.[14] If the Polanyi equation is recast in free energy terms [$\Delta G^{\ddagger} = \alpha(\Delta G) + \beta$], then in Marcus theory terminology $\beta = (1/4)\lambda$ (and $\alpha = 0.5 + [\Delta G/2\lambda]$). The intrinsic barriers are often divided into inner-sphere and outer-sphere reorganization energies. For instance, the observation that proton-transfer barriers are much higher for carbon acids and metal hydrides than for nitrogen or oxygen acids has been ascribed to greater inner-shell reorganization energies.[10] The lower reactivity of carbon versus oxygen radicals toward hydrogen atom abstraction is probably due to differences in reorganization energies as well as polar effects.

Studies of self-exchange reactions—reactions that involve degenerate exchange of a particle or group—are a way to directly determine intrinsic barrier heights. Reported here are self-exchange reactions involving iron bi-imidazoline complexes (Chart 1). Nelson and co-workers have described iron(II) and iron(III) complexes of these ligands, [Fe^{II}-2,2′-bi-imidazoline (H$_2$bim)$_3$](ClO$_4$)$_2$ [abbreviated **Fe^{II}(H$_2$bim)**] and [Fe^{III}(H$_2$bim)$_3$]-(ClO$_4$)$_3$ [**Fe^{III}(H$_2$bim)**], as well as an iron(III) complex in which one of the bi-imidazoline ligands is deprotonated, [Fe^{III}(Hbim)-(H$_2$bim)$_2$](ClO$_4$)$_2$ [**Fe^{III}(Hbim)**].[15] We have recently shown that **Fe^{III}(Hbim)** oxidizes hydrocarbons with weak C−H bonds by a mechanism best described as hydrogen atom abstraction.[6] Thus this species serves as a functional model for nonheme iron-containing enzymes that mediate the net transfer of hydrogen atoms. More generally, the bi-imidazoline ligands used here are crude models for histidine residues that are often involved in

enzymatic proton-coupled electron-transfer reactions.[16] This study aims to probe the relation between hydrogen atom transfer and proton-coupled electron transfer, terms that often describe the same overall process with the same ground-state thermodynamics (H• ≡ H+ + e−).

Fe^{II}(H$_2$bim) and **Fe^{III}(H$_2$bim)** differ by an electron, so interconversion of these two species is an electron self-exchange reaction with rate constant k_{e^-} (eq 2). Similarly, **Fe^{III}(H$_2$bim)** plus **Fe^{III}(Hbim)** is a proton self-exchange reaction (k_{H^+}, eq 3). **Fe^{II}(H$_2$bim)** and **Fe^{III}(Hbim)** must exchange both an electron and a proton to interconvert, so eq 4 is a proton-coupled electron transfer or a net hydrogen atom transfer reaction ($k_{H\bullet}$).

$$[\text{Fe}^{II}(\text{H}_2\text{bim})_3]^{2+} + [\text{Fe}^{III}(\text{H}_2\text{bim})_3]^{3+} \underset{k_{e^-}}{\rightleftharpoons}$$
$$[\text{Fe}^{III}(\text{H}_2\text{bim})_3]^{3+} + [\text{Fe}^{II}(\text{H}_2\text{bim})_3]^{2+} \quad (2)$$

$$[\text{Fe}^{III}(\text{H}_2\text{bim})_3]^{3+} + [\text{Fe}^{III}(\text{Hbim})(\text{H}_2\text{bim})_2]^{2+} \underset{k_{H^+}}{\rightleftharpoons}$$
$$[\text{Fe}^{III}(\text{Hbim})(\text{H}_2\text{bim})_2]^{2+} + [\text{Fe}^{III}(\text{H}_2\text{bim})_3]^{3+} \quad (3)$$

$$[\text{Fe}^{II}(\text{H}_2\text{bim})_3]^{2+} + [\text{Fe}^{III}(\text{Hbim})(\text{H}_2\text{bim})_2]^{2+} \underset{k_{H\bullet}}{\rightleftharpoons}$$
$$[\text{Fe}^{III}(\text{Hbim})(\text{H}_2\text{bim})_2]^{2+} + [\text{Fe}^{II}(\text{H}_2\text{bim})_3]^{2+} \quad (4)$$

Hydrogen atom self-exchange has received limited attention. There are a few experimental rate constants for organic radicals (see below)[17] and for metalloradicals plus metal hydride complexes.[18] There are related measurements of comproportionation reactions involving proton-coupled electron transfer (or H• transfer) where $\Delta G°$ is small, most notably involving ruthenium−oxo complexes.[19] Reported here is the first kinetic analysis of net H• self-exchange between metal-bound ligands.[20] Also described is a rare comparison of electron, proton, and H-atom self-exchange rates in the same system, analyses of the intrinsic barriers using a Marcus-theory approach, and comparisons with related transition metal and main group reactions.

Experimental Section

All manipulations were anaerobic using either a N$_2$-filled glove box or vacuum line techniques. The glove box was kept free of reductants (such as phosphines) as well as O$_2$ and H$_2$O. UV/vis spectra were obtained using an HP8452A spectrophotometer. NMR spectra were acquired on Bruker WM-500, DRX-499, AF-300, and AC-200 spectrometers. Temperature calibration of the NMR probes was accomplished by Van Geet's method.[21] Chemical shifts are reported relative to tetramethylsilane.

(9) (a) Savéant, J.-M. In *Advances in Electron Transfer Chemistry*; Mariano, P. S., Ed.; JAI Press: Greenwich, CT, 1991; Vol. 4, p 53. (b) Savéant, J.-M. *Acc. Chem. Res.* **1993**, *26*, 455. (c) For a recent extension of the Savéant model, and a more complete list of references, see Donkers, R. L.; Maran, F.; Wayner, D. D. M.; Workentin, M. S. *J. Am. Chem. Soc.* **1999**, *121*, 7239−7248. (d) For an extension of this model to proton transfer, see ref 10f.

(10) (a) Kramarz, K. W.; Norton, J. R. *Prog. Inorg. Chem.* **1994**, *42*, 1−65. (b) Caldin, E., Gold, V., Eds. *Proton-Transfer Reactions*; Wiley: New York, 1975, especially Crooks, J. E., pp 153−177 and Kresge, A. J., pp 179−199. (c) Kresge, A. J.; *Acc. Chem. Res.* **1975**, *8*, 354−360; *Chem. Soc. Rev.* **1973**, *2*, 475−503. (d) Kristjánsdóttir, S. S.; Norton, J. R. *J. Am. Chem. Soc.* **1991**, *113*, 4366−4367. (e) Reference 8. (f) Anne, A.; Fraoua, S.; Grass, V.; Moiroux, J.; Savéant, J.-M. *J. Am. Chem. Soc.* **1998**, *121*, 2951−2958. (g) Creutz, C.; Sutin, N. *J. Am. Chem. Soc.* **1988**, *110*, 2418.

(11) (a) Lee, K.-W.; Brown, T. L. *J. Am. Chem. Soc.* **1987**, *109*, 3269−3275. (b) Schwarz, C. L.; Endicott, J. F. *Inorg. Chem.* **1995**, *34*, 4572. (c) Endicott, J. *Prog. Inorg. Chem.* **1983**, *30*, 141. (d) Anderson, K. A.; Kirchner, K.; Dodgen, H. W.; Hunt, J. P.; Wherland, S. *Inorg. Chem.* **1992**, *31*, 2605−8. (e) Shea, T. M.; Deraniyagala, S. P.; Studebaker, D. B.; Westmoreland, T. D. *Inorg. Chem.* **1996**, *35*, 7699−7703. (f) Abu-Omar, M. M.; Appelman, E. H.; Espenson, J. H. *Inorg. Chem.* **1996**, *35*, 7751−7.

(12) Lee, I.-S. H.; Jeoung, E. H.; Kreevoy, M. M. *J. Am. Chem. Soc.* **1997**, *119*, 2722−2728.

(13) (a) Reference 8f and references therein. (b) Skoog, S. J.; Gladfelter, W. L. *J. Am. Chem. Soc.* **1997**, *119*, 11049−11060. (c) Pellerite, M. J.; Brauman, J. I. *J. Am. Chem. Soc.* **1983**, *105*, 2672−2680.

(14) References 8a, b. (b) For a nice overview, see Shaik, S. S.; Schlegel, H. B.; Wolfe, S. *Theoretical Aspects of Physical Organic Chemistry: The S$_N$2 Mechanism*; Wiley: New York, 1992; Chapter 1.

(15) (a) Burnett, M. G.; McKee, V.; Nelson, S. M. *J. Chem. Soc., Dalton Trans.* **1981**, 1492−1497. (b) Wang, J. C.; Bauman, J. E., Jr. *Inorg. Chem.* **1965**, *4*, 1613−1615.

(16) The oxidation of tyrosine Z in photosystem II is a much-studied example; for leading references, see: (a) Tommos, C.; Babcock, G. T. *Acc. Chem. Res.* **1998**, *31*, 18−25. (b) Hays, A. M.; Vassilieu, I. R.; Golbeck, J. H.; Debus, R. J. *Biochemistry* **1998**, *37*, 11352−11365. (c) Christen, G.; Renger, G. *Biochemistry* **1999**, *38*, 2068−2077.

(17) (a) Camaioni, D. M.; Autrey, S. T.; Salinas, T. B.; Franz, J. A. *J. Am. Chem. Soc.* **1996**, *118*, 2013−2022. (b) See Table 4 and references therein.

(18) (a) Cooley, N. A.; Watson, K. A.; Fortier, S.; Baird, M. C. *Organometallics* **1986**, *5*, 2563−2564. (b) Song, J.; Bullock, R. M.; Creutz, C. *J. Am. Chem. Soc.* **1991**, *113*, 9862−9864. (c) Protasiewicz, J. D.; Theopold, K. H. *J. Am. Chem. Soc.* **1993**, *115*, 5559−5569. (d) Kiss, G.; Zhang, K.; Mukerjee, S. L.; Hoff, C. D. *J. Am. Chem. Soc.* **1990**, *112*, 5657−8.

(19) (a) Binstead, R. A.; Meyer, T. J. *J. Am. Chem. Soc.* **1987**, *109*, 3287−3297. (b) Farrer, B. T.; Thorp, H. H. *Inorg. Chem.* **1999**, *38*, 2497−2502. (c) References 2c and 5c.

(20) A Marcus analysis of interconversion of (H$_2$O)$_5$CrOO^{2+} and (H$_2$O)$_5$-CrOOH^{2+} is given in Kang, C.; Anson, F. C. *Inorg. Chem.* **1994**, *33*, 2624−2630.

(21) Van Geet, A. L. *Anal. Chem.* **1968**, *40*, 2227−2229.

Reagents were purchased from Aldrich and purified by standard procedures[22] unless otherwise noted. Acetonitrile (Burdick and Jackson, low-water brand) was stored in an argon-pressurized stainless steel drum, and used as received via a stainless steel dispensing system plumbed directly into the glove box. Piperidine and *N*-methylmorpholine were distilled from sodium. Ethylenediamine, tetra-*n*-butylammonium perchlorate, quinuclidine, 1,8-diazo-bicyclo[5.4.0.]undec-7-ene (DBU) (Fluka), silver perchlorate (Alfa), dithiooxamide, and bromoethane were used as received. Quinuclidinium perchlorate and H(DBU)-ClO_4 were prepared by addition of 70% perchloric acid to ethereal solutions of the bases. Precipitates were washed with diethyl ether and dried under reduced pressure in a steel vessel. (***Caution: Perchlorate salts are potentially explosive***). Deuterium-enriched reagents were purchased from Cambridge Isotope Laboratories. Ethylenediamine-d_4 ($H_2NCD_2CD_2NH_2$), methanol-d_4, methanol-O*D*, and ethanol-d_6 were used as received. Dimethyl sulfoxide (DMSO)-d_6 was dried over 4-Å molecular sieves. Acetonitrile (MeCN)-d_3 was dried over calcium hydride followed by phosphorus pentoxide, and the cycle repeated until the H_2O content was ≤2 mM as determined by ^{1}H NMR using $(Me_3Si)_2O$ as an internal standard.

Syntheses of $[Fe^{II}(H_2bim)_3](ClO_4)_2$ [abbreviated **$Fe^{II}(H_2bim)$**], $[Fe^{III}(H_2bim)_3](ClO_4)_3$ [**$Fe^{III}(H_2bim)$**], and $[Fe^{III}(Hbim)(H_2bim)_2]$-$(ClO_4)_2$ [**$Fe^{III}(Hbim)$**] followed the published procedures.[15] Purity of the materials was checked by optical spectroscopy, pH and redox titrations, and ^{1}H NMR (for diamagnetic impurities such as H_2bim). ^{1}H NMR spectra for the iron complexes are described in Results. Elemental analyses were performed by Canadian Microanalytical Service (Delta, BC) and Atlantic Microlabs (Norcross, GA). Analytical data: Calcd for $C_{18}H_{30}$-$Cl_2FeO_8N_{12}$ [**$Fe^{II}(H_2bim)$**]: C, 32.27; H, 4.48; N, 25.10. Found: C, 32.35; H, 4.48; N, 24.82. Calcd for $C_{18}H_{30}Cl_3$-$FeN_{12}O_{12}$ [**$Fe^{III}(H_2bim)$**]: C, 28.10; H, 3.94; N, 21.85. Found: C, 28.61; H, 4.05; N, 21.89. Calcd for $C_{18}H_{29}Cl_2FeN_{12}O_8$ [**Fe^{III}-(Hbim)$**]: C, 32.32; H, 4.38; N, 25.14. Found: C, 32.43; H, 4.47; N, 24.85. 2,2′-Bi-imidazoline-d_8 (each methylene CD_2) was prepared by the reported procedure[15b] using ethylenediamine-d_4, and this ligand was used to prepare the deuterated iron complexes **$Fe^{II}(H_2bim)$-d_{24}** and **$Fe^{III}(H_2bim)$-d_{24}**. Deuterium was incorporated into the amine positions by repeated dissolution in methanol−O*D* and removal of solvent, enabling the preparations of **$Fe^{II}(D_2bim)$-d_6**, **$Fe^{III}(D_2bim)$-d_6**, **$Fe^{II}(D_2bim)$-d_{30}**, and **$Fe^{III}(D_2bim)$-d_{30}**. **$Fe^{III}(Dbim)$-d_5**, **$Fe^{III}(Hbim)$-d_{24}**, and **$Fe^{III}(Dbim)$-d_{29}** were directly synthesized from the iron(II) analogues. Enrichment ranged from 80 to 98% as judged by ^{1}H and ^{2}H NMR.

Magnetic moments were determined by the Evans method[23] at 500 MHz and 298 K. CD_3CN and $(Me_3Si)_2O$ were used as solvent and standard, respectively. The concentrations of internal and external standards were identical and close to that of the paramagnetic analyte. In none of the experiments did the signal due to the internal standard broaden. The reported moments are corrected for the diamagnetic susceptibilities of the solvent,[24] ligands ($104 × 10^{-6}$ cgs), ClO_4^- ($34 × 10^{-6}$ cgs), and Fe^{2+} ($13 × 10^{-6}$ cgs) or Fe^{3+} ($10 × 10^{-6}$ cgs) ions.[15b,25]

Cyclic voltammetry measurements were made using a BAS CV-27. The cell consisted of analyte-containing solution (5−

10 mM) in acetonitrile (0.1 M *n*-Bu_4NPF_6), an Ag/$AgNO_3$ reference electrode, a platinum disk working electrode, and a platinum wire auxiliary electrode. Ferrocene was used as an internal standard. Square-wave voltammetry was performed by R. LeSuer and W. Geiger at the University of Vermont. All measurements were carried out in a nitrogen-filled glove box at room temperature. Acidity constants were evaluated by quantification of the iron species present at varying concentrations of added nitrogenous base using optical spectroscopy, NMR spectroscopy, or cyclic voltammetry.

Kinetic measurements were made by ^{1}H and ^{2}H NMR spectroscopies. Samples were freshly prepared in resealable (J-Young's brand) NMR tubes in the glove box and their concentrations checked by optical spectroscopy. Tubes were equilibrated in the NMR probe for 10−15 min before recording spectra. At least 120 scans were acquired. Data sets of 16K and 32K were zero-filled before Fourier transforming. Signals were fit to Lorenzian functions using the commercially available NUTS software (Acorn NMR), with residuals typically less than 10%. In the slow exchange regime, pseudo-first-order rate constants were obtained by subtracting the full widths at half-maximum (fwhm) in the absence of exchange from that of the exchange-broadened signals at a given temperature. The natural line widths of **$Fe^{II}(H_2bim)$** and **$Fe^{III}(H_2bim)$** were calibrated in each experiment. Samples were checked for decomposition after acquisition of kinetic data. Rate measurements were identical within experimental error before and after sample heating. Bimolecular rate constants and activation parameters were derived from linear least-squares analysis using Kaleida-Graph (Synergy Software). Errors are reported as two standard deviations about the mean (2σ). In the intermediate exchange regime, rates were determined by simulation of the population-weighted NH signal. Dynamics simulations were performed using the commercially available software package gNMR version 4.1 (Cherwell Scientific).

Crystallographic data for the X-ray structures of **$Fe^{II}(H_2bim)$**, **$Fe^{III}(H_2bim)$**, and **$Fe^{III}(Hbim)$** can be found in Table 1; Table 2 lists selected bond lengths and angles. Diffraction data were collected using a Nonius Kappa CCD with Mo Kα radiation. Crystals were mounted on glass pins with epoxy or oil. Nonhydrogen atoms were refined anisotropically by a full-matrix least-squares method. All intensities were integrated and subsequently scaled with the Denzo-SMN package.[26] Hydrogen atoms were located from difference maps and refined with a riding model, except as noted.

Red plates of **$Fe^{II}(H_2bim)$** were obtained by slow evaporation of an acetone/*o*-dichlorobenzene solution at room temperature under an atmosphere of nitrogen. Normalized structure factors indicated a center of symmetry favoring the centrosymmetric space group *C*2/*c* (no. 15) over Cc (no. 9). Disorder due to large librational motion at N(6) along a vector perpendicular to the plane of the ring was modeled by assigning two discrete sites [N(6) and N(6a)] along this vector and assigning 0.5 occupancy to each site. Orange plates of **$Fe^{III}(H_2bim)$** were grown by slow cooling of a hot ethanolic solution to room temperature. Disorder at O(11) and O(12) was modeled by splitting these atoms into two discrete sites with 0.5 occupancy. Green plates of **Fe^{III}-(Hbim)$** were obtained over the course of 2 h by placing a degassed solution of **$Fe^{II}(H_2bim)$** in acetonitrile/diethyl ether under an atmosphere of molecular oxygen. This technique of slow diffusion of O_2 at room temperature was reproducible and the only one found to yield X-ray-quality crystals. All protons

(22) Perrin, D. D.; Armarego, W. L. F. *Purification of Laboratory Chemicals,* 3rd ed.; Pergamon: New York, 1988.

(23) (a) Sur, S. K. *J. Magn. Reson.* **1989**, *82,* 169−173. (b) Live, D. H.; Chan, S. I. *Anal. Chem.* **1970**, *42,* 791−792.

(24) Gerger, W.; Mayer, U.; Gutmann, V. *Monatsh. Chem.* **1977**, *108,* 417−422.

(25) O'Connor, C. J. *Prog. Inorg. Chem.* **1982**, *29,* 203−283.

(26) Otinowski, Z.; Minor, W. *Methods Enzymol.* **1996**, *276,* 307−326.

Table 1. X-Ray Diffraction Data

complex	[Fe^{II}(H$_2$bim)]	[Fe^{III}(H$_2$bim)]	[Fe^{III}(Hbim)]
empirical formula	C$_{18}$H$_{30}$Cl$_2$FeO$_8$N$_{12}$	C$_{18}$H$_{30}$Cl$_3$FeO$_{12}$N$_{12}$	C$_{18}$H$_{29}$Cl$_2$FeO$_8$N$_{12}$
FW	669.29	768.74	668.28
crystal system	monoclinic	monoclinic	orthorhombic
space group	C2/c	P2$_1$/c	Pca2$_1$
unit cell dimensions	a = 13.3079 (3)	a = 17.5362 (15)	a = 13.2140 (2)
(Å, deg)	b = 13.5922 (4)	b = 14.1422 (10)	b = 13.4070 (3)
	c = 16.1716 (4)	c = 12.580 (2)	c = 15.7310 (3)
	β = 108.5820 (2)	β = 90.450 (4)	
volume (Å^3)	2772.68 (12)	3119.8 (6)	2786.91 (9)
Z	4	4	4
density (g/cm^3, calcd)	1.603	1.637	1.593
μ (mm^{-1})	0.803	0.817	0.799
λ (Å)	0.71070	0.71070	0.71070
crystal size (mm)	0.38 × 0.23 × 0.16	0.11 × 0.05 × 0.03	0.28 × 0.19 × 0.04
temperature (K)	300 (2)	161 (2)	298 (2)
θ range (deg)	2.66−28.28	2.17−20.90	2.16−30.50
index ranges	−16 ≤ h ≤ 16,	−17 ≤ h ≤ 17,	−17 ≤ h ≤ 16,
	−18 ≤ k ≤ 18,	−14 ≤ k ≤ 14,	−19 ≤ k ≤ 19,
	−21 ≤ l ≤ 21	−12 ≤ l ≤ 12	−22 ≤ l ≤ 22
reflections collected	47 314	27 013	63 346
unique reflections	3147	3288	7807
R$_{int}$	0.032	0.085	0.048
parameters refined	195	433	371
final R, R$_w$ (I > 2σI)	0.0742, 0.2315	0.0635, 0.1845	0.0504, 0.1619
goodness of fit	1.096	1.154	1.030

Table 2. Selected Bond Lengths (Å) and Angles (deg)

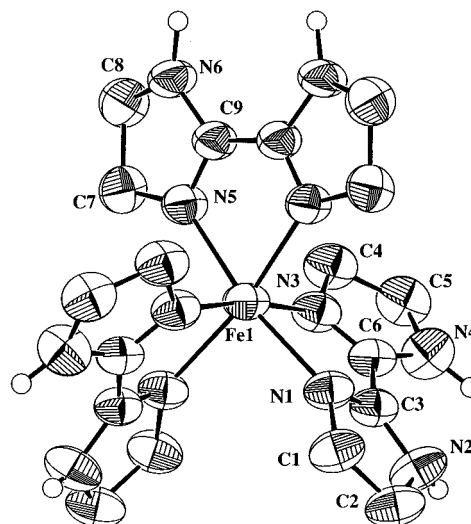|	Fe^{II}(H$_2$bim)	Fe^{III}(H$_2$bim)	Fe^{III}(Hbim)
Fe−N(1)	2.172 (3)	2.090 (7)	2.121 (3)
Fe−N(3)	2.198 (4)	2.080 (7)	2.076 (3)
Fe−N(5)	2.167 (3)	2.085 (7)	2.121 (4)
Fe−N(7)		2.075 (7)	2.005 (4)^a
Fe−N(9)		2.079 (7)	2.151 (4)
Fe−N(11)		2.064 (7)	2.084 (3)
∠ N(1)−Fe−N(3)	75.7 (1)	77.3 (3)	77.0 (1)
∠ N(5)−Fe−N(7)	76.4 (2)^b	77.2 (3)	78.4 (2)
∠ N(9)−Fe−N(11)		77.7 (3)	76.5 (1)
∠ N(1)−Fe−N(7)		165.3 (3)	167.4 (2)
∠ N(3)−Fe−N(11)	171.4 (2)^c	163.1 (3)	164.4 (2)
∠ N(5)−Fe−N(9)	166.6 (1)^d	167.3 (3)	164.3 (1)

^{a} N(7) is in the same imidazoline ring as the deprotonated nitrogen, N(8). ^{b} ∠ N(5)−Fe−N(5A). ^{c} ∠ N(3)−Fe−N(3A). ^{d} ∠ N(1)−Fe−N(5).

were located from difference maps except those on C(7), C(8), C(13), and N(12), which were placed with ideal geometries.

Results

1. Characterization. Syntheses, optical spectra, and solid-state magnetic properties of **Fe^{II}(H$_2$bim)**, **Fe^{III}(H$_2$bim)**, and **Fe^{III}(Hbim)** have been reported.[15] Our measurements of magnetic moments by the Evans method confirm the high-spin nature of all three compounds in acetonitrile solution at 298.2 K. The μ_{eff} values of 5.8 and 5.9 μ_B for **Fe^{III}(H$_2$bim)** and **Fe^{III}-(Hbim)** are close to the spin-only value of 5.92 μ_B for an S = 5/2 ground state. For **Fe^{II}(H$_2$bim)**, the μ_{eff} of 5.0 μ_B is close to the spin-only value for S = 2, 4.90 μ_B, as is common for high-spin ferrous complexes.[27]

X-ray crystal structures of the three compounds support the high-spin assignments (Figures 1−3, Tables 1, 2). Each of the iron complexes is pseudo-octahedral, distorted by the narrow bite angle of the H$_2$bim ligand: 76.0 ± 0.4° for **Fe^{II}(H$_2$bim)**, 77.4 ± 0.3° for **Fe^{III}(H$_2$bim)**. The smaller bite angle for the ferrous complex is the result of its longer Fe−N bond lengths of 2.18 ± 0.02 Å, versus 2.08 ± 0.02 Å for **Fe^{III}(H$_2$bim)**. These

(27) Figgis, B. N. *Introduction to Ligand Fields*; Wiley-Interscience: New York 1966; pp 267−290.

Figure 1. ORTEP drawing of the cation in [Fe^{II}(H$_2$bim)$_3$][ClO$_4$]$_2$ [**Fe^{II}-(H$_2$bim)**].

bond lengths, and the 0.1 Å difference between them, are typical of octahedral high-spin iron complexes with nitrogen ligands.[28] In all the structures the bi-imidazoline ligands are essentially planar with N−C−C−N torsion angles of <0.06°, with the exception of the bi-imidazoline ligand of **Fe^{II}(H$_2$bim)** containing disordered N(6). The two imidazoline rings of each ligand are bent toward each other to accommodate the iron: for instance, the N(1)−C(3)−C(6) versus N(2)−C(3)−C(6) angles are 116.7 ± 1° versus 126.3 ± 1° in the three structures.

In the structures of **Fe^{II}(H$_2$bim)** and **Fe^{III}(H$_2$bim)**, each of the NH groups hydrogen-bonds to a perchlorate counterion. Many of these appear to be bifurcated hydrogen bonds, with the hydrogen close to two perchlorate oxygen atoms.[29] The mean

(28) (a) Mikami, M.; Konno, M.; Saito, Y. *Acta Crystallogr., Sect. B* **1980**, *36*, 275−287. (b) Oliver, J. D.; Mullica, D. F.; Hutchinson, B. B.; Milligan, W. O. *Inorg. Chem.* **1980**, *19*, 165−169. (c) Boinnard, D.; Cassoux, P.; Petrouleas, J.-M.; Tuchagues, J.-P. *Inorg. Chem.* **1990**, *29*, 4114−4122. (d) Lorente, M. A. M.; Dahan, F.; Sanakis, Y.; Petrouleas, V.; Bousseksou, A.; Tuchagues, J.-P. *Inorg. Chem.* **1995**, *34*, 5346−5357.
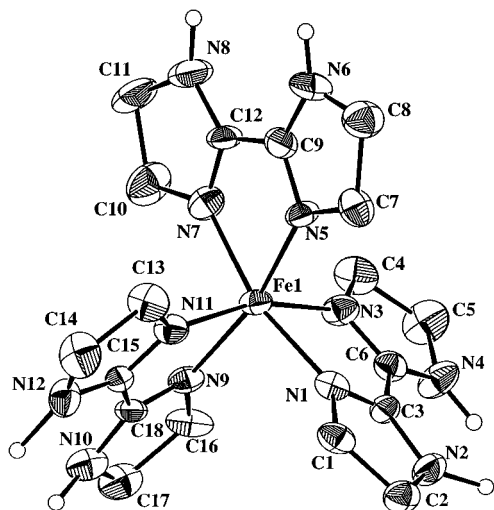
Figure 2. ORTEP drawing of the cation in [Fe^{III}(H_2bim)$_3$][ClO_4]$_3$ [**Fe^{III}-(H_2bim)**].
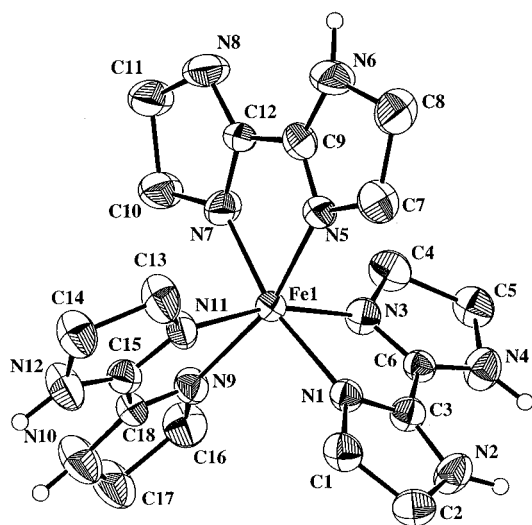
Figure 3. ORTEP drawing of the cation in [Fe^{III}(Hbim)(H_2bim)$_2$]-[ClO_4]$_2$ [**Fe^{III}(Hbim)**].

N···O distance of 3.02 Å [range: 2.89 (1)−3.17 (3) Å] and NH···O angles of 117−170° are typical of NH···O bonds and bifurcated hydrogen bonds.[29a] The hydrogen bond network of **Fe^{III}(Hbim)** (Figure 4) is different in that one NH group hydrogen-bonds to the deprotonated nitrogen of another cation. The distance between N(8) and N(12) of the adjacent hydrogen bond donor is 2.673 (4) Å with ∠N−H···N = 162°, indicating a rather strong hydrogen bond.[30] The Fe−N bond lengths of **Fe^{III}(Hbim)** range from 2.005 (4) to 2.151 (4) Å, flanking the Fe−N bond lengths in **Fe^{III}(H_2bim)**, which average 2.08 Å. The shortest Fe−N bond [to N(7)] is to the deprotonated imidazoline ring, as expected. The Fe···Fe distance across the NH···N interaction is 10.3 Å.

The ^{1}H NMR spectrum of **Fe^{II}(H_2bim)** (Figure 5) is paramagnetically shifted, with resonances at δ 10.7 (12 C*H*), δ 24.6 (12 C*H*), and δ 46.1 (6 N*H*). The N*H* resonances were assigned by their disappearance on exchange with methanol-OD. The

(29) The structural data are consistent with the solid-state infrared spectra described in ref 15a. (a) Bifurcated H-bonds: Jeffrey, G. A. *An Introduction to Hydrogen Bonding;* Oxford University Press: New York, 1997; pp 70−71.

(30) (a) Reference 29a. (b) Benedict, H.; Limbach, H. H.; Wehlan, M.; Fehlhammer, W. P.; Golubev, N. S.; Janoschek, R. *J. Am. Chem. Soc.* **1998**, *120*, 2939−2950. (c) Perrin, C. L.; Nielson, J. B. *Annu. Rev. Phys. Chem.* **1997**, *48*, 511−544.
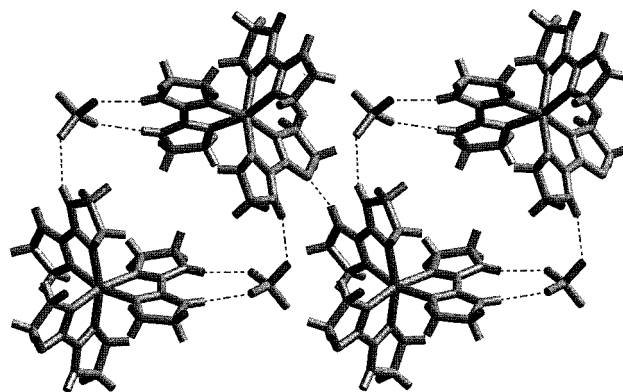

Figure 4. Drawing of [Fe^{III}(Hbim)(H_2bim)$_2$][ClO_4]$_2$ [**Fe^{III}(Hbim)**], showing hydrogen bonds as dashed lines between imidazoline NH groups and perchlorate counterions or the deprotonated imidazoline.
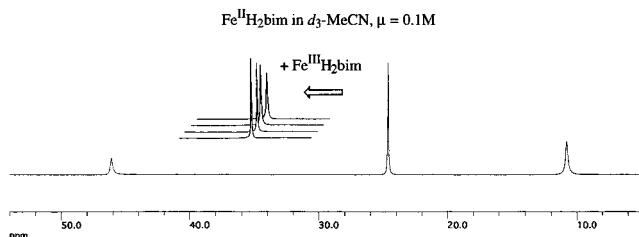

Figure 5. Line-broadening of **Fe^{II}(H_2bim)** with added **Fe^{III}(H_2bim)**. Only the broadening of the δ 24.6 resonance is shown.

signals fit well to Lorenzian functions with fwhm of 30 Hz (δ 24.6), 105 Hz (δ 10.8), and ca. 75 Hz (δ 46.1). The line widths correspond to effective T_2 relaxation times at 298 K of 11, 3, and ca. 4 ms, respectively. The spectrum is independent of magnetic field strength from 200 to 500 MHz. Increasing the temperature from 278 to 374 K causes the signals to shift toward the diamagnetic region and broaden. The inverse relation between temperature and shift is characteristic of Curie paramagnets, whereas the increase in line width with temperature, although not unusual, has a more complex nature.[31] The ^{2}H NMR spectra of **Fe^{II}(H_2bim)-d_{24}** and **Fe^{II}(D_2bim)-d_{30}** are significantly sharper than the proton spectrum, with Lorenzian signals at δ 10.5 (14 Hz), δ 24.7 (13 Hz), and δ 45.8 (62 Hz). Deuterium spectra of paramagnets can be as much as 42 times sharper than analogous proton spectra (the square of the ratio of nuclear gyromagnetic constants of H and D), but the full effect is rarely observed and the spectral resolution is partially balanced by the 6.5-fold decrease in chemical shift dispersion in the ^{2}H spectrum.[31a] In the ^{13}C NMR, three signals were discerned at δ 465.8 (CH$_2$, t, $^1J_{C-H} \approx$ 138 Hz), δ −76.8 (*C*=N, s, fwhm ≈ 100 Hz), and δ −242 (CH$_2$, broad fwhm ≈ 310 Hz). Heteronuclear magnetic quantum coherence experiments showed a cross-peak between the ^{13}C resonance at δ 465.8 and the ^{1}H resonance at δ 24.6 (^{1}H), but rapid relaxation apparently precluded observation of other signals.

The observation of only two methylene resonances is inconsistent with a static structure of effective D_3 symmetry, as seen in the solid state and as expected for octahedral M(L−L)$_3$ compounds. Such structures are chiral, so each CH$_2$ group is a diastereotopic pair. A spectrum indicative of D_3 symmetry is found for the analogous cobalt(III) ion, [Co(H_2bim)$_3$]$^{3+}$, which

(31) (a) LaMar, G. N.; Horrocks, W. D., Jr.; Holm, R. H. *NMR of Paramagnetic Molecules: Principles and Applications*; Academic Press: New York, 1973. (b) Bertini, I.; Luchinat, C. *NMR of Paramagnetic Molecules in Biological Systems*; Benjamin/Cummings: Menlo Park, CA, 1986.

is diamagnetic (low-spin d[6]).[32] **Fe^{II}(H$_2$bim)** must be undergoing a fluxional process that equilibrates two pairs of hydrogens. Lowering the temperature to 260 K did not cause decoalescence of the ^{1}H NMR spectrum. Because all of the peak shapes are Lorenzian, the fluxional process is fast with respect to the NMR time scale. Most likely, the fluxional process is racemization of the iron center via dissociation of one arm of a bi-imidazoline ligand. [Fe^{II}(bipy)$_3$]$^{2+}$ undergoes such racemization, but on a much slower time scale ($t_{1/2}$ = 18 min) because the iron is low-spin.[33] The related cobalt(II) complex [Co(H$_2$bim)$_3$]$^{2+}$ has a proton spectrum similar to that of **Fe^{II}(H$_2$bim)**, as does the nickel derivative [Ni(H$_2$bim)$_3$]$^{2+}$ at 343 K, but at ambient temperatures one of the signals for the nickel complex has decoalesced.[32] This is consistent with thermally activated site exchange and the lower lability of Ni^{2+} versus high-spin Fe^{2+}. Complete dissociation of the bi-imidazoline ligand from **Fe^{II}-(H$_2$bim)** is not fast with respect to the NMR time scale, evidenced by the fact that resonances for added free ligand are observed in solutions containing >30 mM **Fe^{II}(H$_2$bim)**. The ligand C*H* resonance (δ 3.7), although broader and slightly shifted in the presence of **Fe^{II}(H$_2$bim)**, does not vary linearly with added iron. **Fe^{II}(H$_2$bim)** does rapidly incorporate uncomplexed H$_2$bim-d_8, an NMR tube reaction being >90% complete within 10 min. Studies of the ligand exchange were hampered by the low solubility (2 mM) of the free ligand in acetonitrile.

NMR signals for the ferric complexes are substantially broader than those of the ferrous complex. The ^{1}H spectrum of **Fe^{III}(H$_2$bim)** consists of signals at δ 37 (6 N*H*, ≈1200 Hz) and δ 130−140 (24 C*H*, ≈3300 Hz). The ^{2}H NMR of **Fe^{III}-(D$_2$bim)-d_{30}** is about 20 times sharper, revealing δ 36.5 (6 N*D*, ≈55 Hz) and a complex multiplet centered at δ 140 for the aliphatic signals. ^{2}H NMR is particularly useful for the deprotonated complex **Fe^{III}(Dbim)-d_{29}**, with resonances at δ 44.5 (5 N*D*, 121 Hz), δ 84.3 (4 C*D*, 108 Hz), δ 164.7 (8 C*D*, 246 Hz), and δ 204−211 (overlapping signals 8 C*D*, 206 Hz), leaving four deuterons undetected. In the ^{1}H NMR, only resonances at δ 40 (5 N*H*, ≈2400 Hz) and δ 80 (4 C*H*, ≈2000 Hz) are barely discernible.

2. Ground-State Energetics. Cyclic voltammograms of **Fe^{II}-(H$_2$bim)** and **Fe^{III}(H$_2$bim)** (in MeCN with 0.1 M *n*-Bu$_4$NPF$_6$) show a single redox couple at −0.31 ± 0.05 V versus FeCp$_2$$^{+/o}$ (internally referenced). The ratio of the anodic to cathodic currents (i_a/i_c) is close to one, indicating chemical reversibility. The current ratio and peak-to-peak separation (120 mV) were independent of scan rate from 50 to 200 mV s^{-1}, and the latter was similar to that of Cp$_2$Fe in the same solution.

The acidity constant (K_a) of **Fe^{III}(H$_2$bim)** was determined electrochemically by oxidizing **Fe^{II}(H$_2$bim)** in the presence of variable amounts of *N*-methylmorpholine.[34] Addition of base resulted in a diminution of the return (cathodic) current, which was the same irrespective of scan rate. This indicates that the protic equilibrium **Fe^{III}(H$_2$bim)** + *N*-methylmorpholine is established on the time scale of the return sweep. The dependence of i_a/i_c on base concentration gave pK_a[**Fe^{III}-(H$_2$bim)**] = 17.5 ± 0.5.[35] These measurements were confirmed by optical spectra of the clean conversion of **Fe^{III}(H$_2$bim)** to **Fe^{III}(Hbim)** on addition of *N*-methylmorpholine, which was reversed on addition of HClO$_4$. These measurements at μ =

0.1 M and ≈1 mM iron gave pK_a values in agreement with the electrochemical result. **Fe^{III}(Hbim)** can itself be deprotonated, with tight isosbestic points observed upon addition of excess quinuclidine indicating a pK_a of 20.5. Back-titration with HClO$_4$ also shows clean isosbestic points. The doubly deprotonated complex, abbreviated **Fe^{III}(bim)**, appears to be stable (λ_{max} = 630 nm, ϵ = 1.1 × 10^4 M^{-1} cm^{-1} in MeCN). **Fe^{III}(bim)** generated by deprotonation of **Fe^{III}(Hbim)** is spectroscopically identical to that produced by the reaction of **Fe^{II}(H$_2$bim)** with O$_2$ in the presence of excess piperidine or quinuclidine. Attempts to further characterize this species by ^{1}H NMR and ^{2}H NMR were unsuccessful because of its low solubility (ca. 3 mg mL^{-1}) and very broad signals. Although not isolable in analytically pure form, **Fe^{III}(bim)** can be reasonably assigned as [Fe(Hbim)$_2$-(H$_2$bim)](ClO$_4$) or [Fe(bim)(H$_2$bim)$_2$](ClO$_4$).

The conversion of **Fe^{II}(H$_2$bim)** to **Fe^{III}(Hbim)** involves removal of an electron [$E°$ for **Fe$^{III/II}$(H$_2$bim)**] and a proton [the pK_a of **Fe^{III}(H$_2$bim)**]. Using a well-established thermochemical cycle,[36] these values give the enthalpy for removal of H• from **Fe^{II}(H$_2$bim)** as 76 ± 2 kcal mol^{-1}.[6] This is the N−H bond strength in **Fe^{II}(H$_2$bim)**. To convert from free energy measurements ($E°$, K_a) to an enthalpy, it is assumed that the entropy difference between **Fe^{II}(H$_2$bim)** and **Fe^{III}(Hbim)** is negligible.[36] Conversion of **Fe^{II}(H$_2$bim)** to **Fe^{III}(Hbim)** can also be accomplished by initial deprotonation to [Fe^{II}(Hbim)(H$_2$bim)$_2$]-ClO$_4$ (abbreviated [**Fe^{II}(Hbim)**]), followed by oxidation. Because the thermochemistry of **Fe^{II}(H$_2$bim)** → **Fe^{III}(Hbim)** is independent of the pathway, the properties of the deprotonated ferrous complex [**Fe^{II}(Hbim)**] are constrained by eq 5 (the factors of 1.37 and 23.1 convert pK_a and $E°$ values to $\Delta G°$ in kcal/mol at 298 K).

$$1.37\{\text{p}K_a[\textbf{Fe}^{\textbf{II}}(\textbf{H}_2\textbf{bim})] - \text{p}K_a[\textbf{Fe}^{\textbf{II}}(\textbf{H}_2\textbf{bim})]\} =$$
$$23.1\{E°[\textbf{Fe}^{\textbf{III/II}}(\textbf{H}_2\textbf{bim})] - E°[\textbf{Fe}^{\textbf{III/II}}(\textbf{Hbim})]\} \quad (5)$$

Measurement of the pK_a of **Fe^{II}(H$_2$bim)** is complicated by the formation of dark blue solids upon deprotonation by stoichiometric DBU or excess *N*-methylmorpholine, tri-*n*-butylamine, piperidine, or quinuclidine. Formation of dark precipitates in the pale red solution occurs several seconds after mixing. Dilution of the sample did not result in dissolution of the precipitate. However, addition of anhydrous triflic acid under an N$_2$ atmosphere regenerated **Fe^{II}(H$_2$bim)**, suggesting the insoluble solids contain [**Fe^{II}(Hbim)**]. Presumably [**Fe^{II}(Hbim)**] aggregates with strong NH⋯N hydrogen bond interactions such as those observed in the solid-state structure of **Fe^{III}(Hbim)**. A lower limit of 23.5 for the pK_a of **Fe^{II}(H$_2$bim)** was estimated by addition of excess piperidine to samples of **Fe^{II}(H$_2$bim)** until change was detected optically or by ^{1}H NMR. Electrochemical reduction of **Fe^{III}(Hbim)** is also not straightforward, possibly because of precipitation of [**Fe^{II}(Hbim)**] on the electrode. The electrode fouling evident in cyclic voltammograms is somewhat less of a problem when using square wave voltammetry. The square wave technique indicates that **Fe^{III}(Hbim)** is roughly 0.5 V harder to reduce than **Fe^{III}(H$_2$bim)**, and that $E°$ [**Fe^{III}-(Hbim)**] ≈ −0.8 V versus Cp$_2$Fe$^{+/o}$. The redox potential implies, via eq 5, that pK_a[**Fe^{II}(H$_2$bim)**] ≈ 26, consistent with the lower bound from direct measurements.

(32) Roth, J. P.; Mayer, J. M. Unpublished results.

(33) Milder, S. J.; Gold, J. S.; Kliger, D. S. *J. Am. Chem. Soc.* **1986**, *108*, 8295−8296.

(34) Following the procedure described in Baldwin, M. J.; Pecoraro, V. L. *J. Am. Chem. Soc.* **1996**, *118*, 11325−11326.

(35) pK_a values for nitrogen bases: Izutsu, K. *Acid−Base Dissociation Constants in Dipolar Aprotic Solvents, IUPAC Chemical Data Series (No. 35);* Blackwell Scientific: London, 1990.

(36) (a) Parker, V. D.; Handoo, K. L.; Roness, F.; Tilset, M. *J. Am. Chem. Soc.* **1991**, *113*, 7493−7498. For related cycles and their application, see (b) Bordwell, F. G., et al. *J. Am. Chem. Soc.* **1991**, *113*, 9790. (b) ibid., **1996**, *118*, 8777. (c) ibid., 10819−10823. (d) Parker, V. D. ibid. **1992**, *114*, 7458 & **1993**, *115*, 1201. (e) Tilset, M.; Parker, V. D. ibid. **1989**, *111*, 6711 and ibid. **1990**, *112*, 2843. (g) Skagestad V.; Tilset, M. ibid. **1993**, *115*, 5077−5083. (i) Wayner, D. D. M.; Lusztyk, E.; Pagé, D.; Ingold, K. U.; Mulder, P.; Laarhoven, L. J. J.; Aldrich, H. S. ibid. **1995**, *117*, 8737.
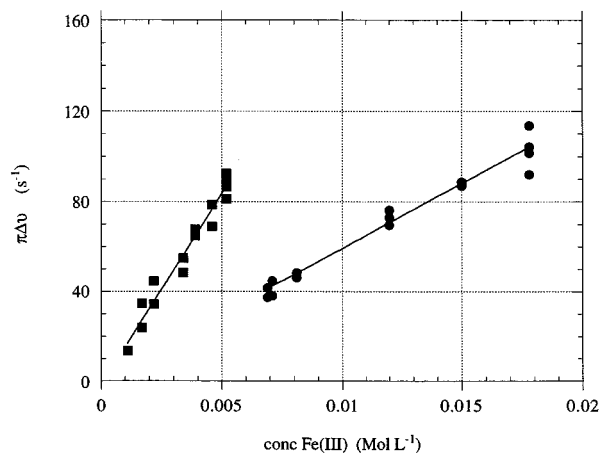
Figure 6. First-order plot for k_{e^-} (squares) and $k_{H^\bullet}$ (circles) in MeCN solution at 298 K.

3. Self-Exchange Rates. Rate constants were determined using dynamic NMR methods.[37] Addition of **$Fe^{III}(H_2bim)$** to solutions of **$Fe^{II}(H_2bim)$** in acetonitrile causes broadening of the resonances for the ferrous complex (Figure 5). The increase in line width, Δv, is proportional to the concentration of **Fe^{III}-(H_2bim)** for both of the CH resonances (Figure 6). The amount of broadening is independent of the concentration of **Fe^{II}-(H_2bim)** and of the spectrometer frequency from 200 to 500 MHz. The broadening caused by the presence of **$Fe^{III}(H_2bim)$** increases with temperature. These observations indicate that **$Fe^{III}(H_2bim)$** and **$Fe^{II}(H_2bim)$** undergo chemical exchange on the ^{1}H NMR time scale. Because these species differ by one electron, this is an electron self-exchange process.

There is no change in chemical shift of the aliphatic signals on addition of **$Fe^{III}(H_2bim)$**, indicating that the reaction is in the slow-exchange limit ($k_{obs} \ll \Delta\delta$ in Hz). In this limit, the broadening is simply related to the rate constant by eq 6,[37] where Δv is the observed increase in fwhm, τ is the lifetime of a nucleus, and k_{obs} is the rate of exchange from this site. k_{obs} is the product of the second-order rate constant k_2 for the chemical reaction times the concentration of the broadening agent X, in this case **$Fe^{III}(H_2bim)$**.

$$\pi\Delta v = \frac{1}{\tau} = k_{obs} = k_2[X] \qquad (6)$$

The slope of the plot of $\pi\Delta v$ versus [**$Fe^{III}(H_2bim)$**] (Figure 6) gives a bimolecular rate constant $k_{e^-} = (1.7 \pm 0.2) \times 10^4$ M^{-1} s^{-1} at 298 K in MeCN-d_3 ($\mu = 0.1$ M), corresponding to a free energy barrier $\Delta G^{\ddagger}$ (298 K) = 11.7 $\pm$ 0.2 kcal mol^{-1}. Activation parameters from rate constants over a 298–355 K range (Figure 7) are $\Delta H^{\ddagger} = 4.1 \pm 0.3$ kcal mol^{-1} and $\Delta S^{\ddagger} = -25 \pm 1$ cal K^{-1} mol^{-1}. The rate is unchanged upon deuteration of the NH groups [**$Fe^{II}(D_2bim)$-d_6** + **$Fe^{III}(D_2bim)$-d_6**]. Solution ionic strength was maintained either by maintaining constant [Fe]$_{total}$ or by addition of n-Bu$_4$NClO$_4$. The rate constants increase approximately two-fold on increasing the ionic strength from 0.1 to 0.4 M. In DMSO-d_6, $k_{e^-} = (6.9 \pm 1.0) \times 10^4$ M^{-1} s^{-1} at 298 K ($\mu = 0.1$ M), a factor of 4 greater than the rate constant in MeCN-d_3.

Addition of **$Fe^{III}(Hbim)$** to solutions of **$Fe^{II}(H_2bim)$** causes qualitatively similar changes in the ^{1}H NMR spectra. Again, the amount of broadening is proportional to the amount of iron-(III) complex added and is the same for the two aliphatic
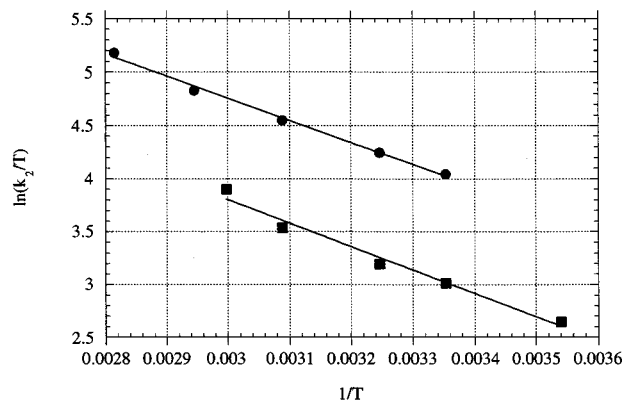
(37) (a) Sandström, J. *Dynamic NMR Spectroscopy*; Academic Press: New York, 1982. (b) Günther, H. *NMR Spectroscopy: Basic Principles, Concepts, and Applications in Chemistry*, 2nd ed.; Wiley: New York, 1992.

Figure 7. Temperature dependence of k_{e^-} (circles) and $k_{H^\bullet}$ (squares) in MeCN solution.

resonances of **$Fe^{II}(H_2bim)$**. As in the previous case, broadening is independent of the concentration of **$Fe^{II}(H_2bim)$** and of the spectrometer frequency (200 to 500 MHz), and the broadening increases with temperature. Because these two complexes differ by a proton and an electron, this is formally a hydrogen atom self-exchange reaction (see below). The rate constant, $k_{H^\bullet} = (5.8 \pm 0.6) \times 10^3$ M^{-1} s^{-1}, is three times slower than k_{e^-} under identical conditions (298 K, $\mu = 0.1$ M); $\Delta G^{\ddagger}$ (298 K) = 12.3 $\pm$ 0.2 kcal mol^{-1}. Eyring analysis (284–333 K) gives $\Delta H^{\ddagger} = 4.4 \pm 0.7$ kcal mol^{-1} and $\Delta S^{\ddagger} = -26 \pm 2$ cal K^{-1} mol^{-1}. The same rate constants are obtained using **$Fe^{II}(H_2bim)$-d_{24}** and **Fe^{III}-($Hbim$)-d_{24}** and measuring the change in CD line widths. In DMSO-d_6, $k_{H^\bullet} = (1.9 \pm 0.2) \times 10^4$ M^{-1} s^{-1} at 298 K, three times faster than the rate in MeCN-d_3, and approximately four times slower than k_{e^-} in the same solvent. A primary kinetic isotope effect k_{NH}/k_{ND} of 2.3 $\pm$ 0.3 was measured at 324 K for the reaction of **$Fe^{II}(D_2bim)$-d_6** and **$Fe^{III}(Dbim)$-d_5**. The same kinetic isotope effect was observed in MeCN-d_3 containing 1–2% ethanol-d_6, added to ensure high deuterium enrichments. In addition, k_{NH}/k_{ND} at 298 K measured using the CD-labeled reactants agreed with measurements on the protio analogues, within experimental error.

The possibility was considered that some **$Fe^{III}(H_2bim)$** present as an impurity in the **$Fe^{III}(Hbim)$** was producing spurious broadening of the **$Fe^{II}(H_2bim)$**. Given that k_{e^-} is only a factor of 3 faster than $k_{H^\bullet}$, ca. 30% of the **$Fe^{III}(Hbim)$** would have to be protonated to account for the broadening observed. N-Methylmorpholine (pK_a = 15.6[35]) added to samples at concentrations up to 2.3 M caused no changes in the formal H$^\bullet$ exchange rates or in the measured isotope effect, although the base would have significantly reduced the concentration of any residual **$Fe^{III}(H_2bim)$**.

The preceding discussion illustrates that although NMR line widths are easily measured, their interpretation needs to be made with care. The results described above are not due to impurities because reproducible rates were obtained between different batches of solvent and iron complexes, with different water concentrations in the solvent, whether **$Fe^{III}(Hbim)$** was isolated or generated in situ with O$_2$, and whether the measurements were done by ^{1}H or ^{2}H NMR. No difference in reactivity was observed between protio MeCN (^{2}H NMR) and MeCN-d_3 (^{1}H NMR), nor did pretreatment of the solvent with copper(II) sulfate as an amine scavenger have an observable effect on the kinetics. Saturation transfer experiments were attempted with the goal of directly demonstrating chemical exchange. Unfortunately, even the deuterated **$Fe^{III}(Hbim)$-d_{24}** has too short a relaxation time to allow measurable magnetization transfer. A number of reagents have been found to broaden the CH signals

Table 3. Kinetic Data for Iron-Bi-imidazoline Self-Exchange Reactions[a]

reaction	k (M⁻¹ s⁻¹)	$\Delta H^{\ddagger}$	$\Delta S^{\ddagger}$	$\Delta G^{\ddagger}$	w_r[b]	$(1/4)\lambda$[c]	$(1/4)\lambda_{outer}$[d]	$(1/4)\lambda_{inner}$[c]
electron transfer (eq 2)	1.7 (± 0.2) × 10⁴	4.1 (± 0.3)[e]	−25 (± 1)[e]	11.7 (± 0.2)	2.1	9.6	4.5	5.1
hydrogen atom transfer (eq 4)	5.8 (± 0.6) × 10³	4.4 (± 0.7)[f]	−26 (± 2)[f]	12.3 (± 0.2)	1.4	10.9	≈0	10.9
proton transfer (eq 3)	≈2 × 10⁶ [g]			9 (± 1)	≈2	≈7		

[a] Values at 298 K, in MeCN-d_3, $\mu = 0.1$ M, in kcal mol⁻¹ ($\Delta H^{\ddagger}$, $\Delta G^{\ddagger}$, w_r, and λ) or cal K⁻¹ mol⁻¹ ($\Delta S^{\ddagger}$). [b] From eqs 8−10. [c] From eq 7. [d] From eq 11. [e] From an Eyring plot over 298−355 K. [f] From an Eyring plot over 284−333 K. [g] Measured values range from 1×10^6 to 4×10^6 M⁻¹ s⁻¹.

of **Fe^{II}(H$_2$bim)**, including 4-nitrophenol (pK_a = 20.7), 2-aminoethanol (17.5), tri-n-butylamine (18.1), piperidine (18.9), quinuclidine (19.5), and DBU (24.3).[38] Even at low concentrations of these reagents {<10 mM, relative to [**Fe^{II}(H$_2$bim)**] ≅ 40 mM}, substantial broadening is observed (10−50 Hz). This is most likely a result of the reagent binding to iron, as more broadening is caused by the sterically unencumbered 2-aminoethanol versus the more crowded piperidine, tri-n-butylamine, and quinuclidine. The broadening does not simply correlate with thermodynamic acidity or basicity. The coordinating acid 4-nitrophenol (pK_a = 20.7) causes broadening, whereas triflic acid, [H-DBU]ClO$_4$ (24.3), and 2,4,6-tri-$tert$-butylphenol (≈28) do not.[39] For the reaction between **Fe^{II}(H$_2$bim)** and **Fe^{III}(Hbim)**, coordination is not the cause of broadening because the doubly deprotonated species **Fe^{III}(bim)**, a more potent base and nucleophile, does not broaden the CH signals of **Fe^{II}(H$_2$bim)**.

Line widths for the NH signals were found to be more susceptible to impurities, so exchange rates were derived from line broadening of the CH signals except in the case of proton self-exchange (see below). Different samples of **Fe^{II}(H$_2$bim)** showed approximately 40% variation in fwhm for the NH sites, substantially larger than the ca. 5% variation in the CH signals. In the electron transfer experiments, rate constants derived from NH broadening agreed with those derived from the CH resonances within a factor of 2. In the H-atom transfer reactions, the NH signals broaden and shift as a function of reactant concentrations and magnetic field strength, indicating chemical exchange in the intermediate rather than slow-exchange regime.

Estimates of the rate constants for proton (and D$^+$) self-exchange (eq 3) were obtained by line-shape analyses of the population, weighted NH or ND signals. Simulation of the exchange-broadened spectra for the reaction of **Fe^{III}(Hbim)** to **Fe^{III}(H$_2$bim)** indicated a second-order rate constant $k_{H^+} \approx 2 \times 10^6$ M⁻¹ s⁻¹ (MeCN-d_3, 298 K, $\mu = 0.1$ M; values ranged from 1×10^6 to 4×10^6 M⁻¹ s⁻¹). This corresponds to a free energy barrier $\Delta G^{\ddagger}$ (298 K) = 9 ± 1 kcal mol⁻¹. Inspection by ^{2}H NMR (30.7 MHz) using the perdeuterated ferric complexes indicated $k_{D^+} \approx 3 \times 10^5$ M⁻¹ s⁻¹ (MeCN, 298 K, $\mu = 0.1$ M). The breadth of the NMR resonances precludes accurate measurements of rate parameters or the kinetic isotope effect. These data suggest that under similar conditions, the proton transfer between iron bi-imidazoline complexes is more facile than both electron and hydrogen atom transfer.
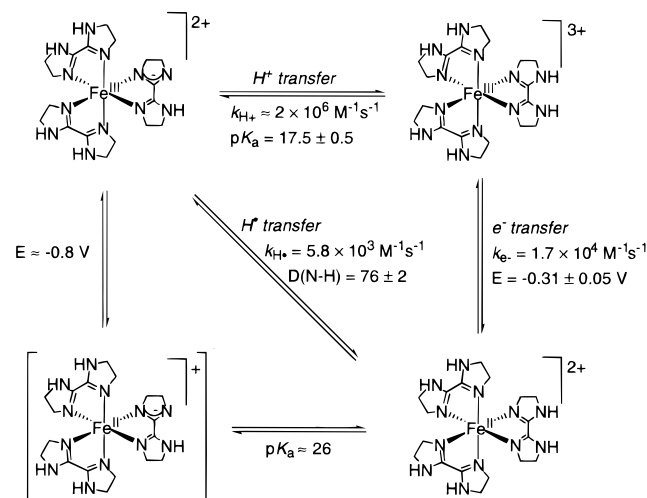
Kinetic and thermodynamic data for the iron bi-imidazoline complexes are summarized in Scheme 1 and Table 3.

Discussion

1. Electron Self-Exchange. The kinetic data for electron transfer between **Fe^{II}(H$_2$bim)** and **Fe^{III}(H$_2$bim)** (Table 3) are

Scheme 1. Thermodynamic and Kinetic Values

H^+ transfer
$k_{H^+} \approx 2 \times 10^6$ M⁻¹s⁻¹
pK_a = 17.5 ± 0.5

$E \approx$ -0.8 V

$H^{\bullet}$ transfer
$k_{H^{\bullet}} = 5.8 \times 10^3$ M⁻¹s⁻¹
D(N-H) = 76 ± 2

e^- transfer
$k_{e^-} = 1.7 \times 10^4$ M⁻¹s⁻¹
$E = -0.31 \pm 0.05$ V

p$K_a \approx 26$

consistent with values for related systems. Self-exchange rates for Fe(phen)$_3$$^{2+/3+}$ and Fe(bipy)$_3$$^{2+/3+}$ are 350 and 220 times faster, with values at 298 K of $k_{e^-} = (6.0 \pm 0.6) \times 10^6$ and $(3.7 \pm 0.8) \times 10^6$ M⁻¹s⁻¹ ($\Delta G^{\ddagger}_{e^-} = 8.2 \pm 0.8$ and 8.5 ± 1.8 kcal mol⁻¹), $\Delta H^{\ddagger}_{e^-} = 2.1 \pm 1.0$ and 2.1 ± 3.0 kcal mol⁻¹, and $\Delta S^{\ddagger}_{e^-} = -21 \pm 3$ and -22 ± 10 cal K⁻¹ mol⁻¹.[40] These measurements were done similarly in acetonitrile by ^{1}H NMR line broadening, although at slightly lower ionic strength (48 and 68 mM, respectively). The lower barriers for Fe(phen)$_3$$^{2+/3+}$ and Fe(bipy)$_3$$^{2+/3+}$ exchange are due to these ions being low-spin, thus undergoing less inner-sphere reorganization on electron transfer. For the low-spin complexes, Fe$^{II/III}$−N distances differ by <0.01 Å,[41] versus ~0.1 Å for Fe(H$_2$bim)$_3$$^{2+/3+}$ (see above). Self-exchange between the high-spin aquo ions Fe(H$_2$O)$_6$$^{2+/3+}$ in aqueous solution ($\mu = 0.55$ M, 294.6 K) is more than a thousand times slower than for Fe(H$_2$bim)$_3$$^{2+/3+}$, with $k_{e^-} = 3.3$ M⁻¹ s⁻¹ ($\Delta G^{\ddagger}_{e^-} = 17$ kcal mol⁻¹), $\Delta H^{\ddagger} = 9.3$ kcal mol⁻¹, and $\Delta S^{\ddagger} = -25$ cal K⁻¹ mol⁻¹.[42] This in part reflects the 0.17 Å change in Fe−O distance on electron transfer.[43]

$\Delta G^{\ddagger}_{e^-}$ for self-exchange is the sum of the work needed to bring the reagents together, w_r, plus the intrinsic barrier $(1/4)\lambda_{e^-}$ (eq 7). The intrinsic barrier is in turn divided into inner-sphere (vibrational, $\lambda_{e^-,i}$) and outer-sphere (solvent, $\lambda_{e^-,o}$) reorganization energies. The work term w_r is the electrostatic repulsion of the ions being brought together and $\lambda_{e^-,o}$ is the solvent reorganization due to the movement of charge on electron transfer. For roughly spherical reagents such as considered here, these can be calculated reasonably accurately according to eqs 8−11.[7] Z_1 and Z_2 are the charges of the ions, D_s and D_o are the static and

(38) pK_a values from ref 35 or Bernasconi, C. F.; Leyes, A. E.; Ragains, M. L.; Shi, Y.; Wang, H.; Wulff, W. D. *J. Am. Chem. Soc.* **1998**, *120*, 8632−8639.

(39) Estimated using the equation pK_a(MeCN) = 7.10 + 1.17pK_a(DMSO) (a) Maran, F.; Celadon, D.; Severin, M. G.; Vianello, E. *J. Am. Chem. Soc.* **1991**, *113*, 9320−9329. (b) Bordwell, F. G. *Acc. Chem. Res.* **1988**, *21*, 456−463. (c) Bordwell, F. G.; Zhang, X.-M. *J. Phys. Org. Chem.* **1995**, *8*, 529−535.

(40) Chan, M. S.; Wahl, A. C. *J. Phys. Chem.* **1978**, *82*, 2542−2549; bipy = 2,2′-bipyridine and phen = 1,10-phenanthroline.

(41) (a) Fujiwara, T.; Iwamoto, E.; Yamamoto, Y. *Inorg. Chem.* **1984**, *23*, 115−117. (b) Johansson, L.; Molund, M.; Oskarrson, Å. *Inorg. Chim. Acta* **1978**, *31*, 117−123.

(42) Silverman, J.; Dodson, R. W. *J. Phys. Chem.* **1952**, *56*, 846−852.

(43) Reference 7d, p 337.

optical dielectric constants of the solvent,[44] r_1 and r_2 are the ionic radii of the reactants, and r_{12} the collision distance. The Debye−Hückel approximation is an accepted treatment reactions at $\mu = 0.1$ M despite deviations from ideal behavior.[45] Equation 9 gives the inverse of the Debye screening factor (f) with Boltzmann's constant (k_B) in kcal K^{-1}, μ in mol dm^{-3}, and the factor 10^{27} to convert dm^3 to Å^3. The term e^2, defined by eq 10 where e_o is the elementary charge, N_A is Avogadro's constant, and ϵ_o is the permittivity of vacuum, is equal to 332.1 kcal Å mol^{-1}.

$$\Delta G^{\ddagger}_{e^-} = w_r + (1/4)\lambda_{e^-} = w_r + (1/4)(\lambda_{e^-,i} + \lambda_{e^-,o}) \quad (7)$$

$$w_r = \frac{e^2 Z_1 Z_2 f}{D_s r_{12}} \quad (8)$$

$$f^{-1} = 1 + r_{12}\sqrt{\frac{8\pi e^2 \mu}{10^{27} D_s k_B T}} \quad (9)$$

$$e^2 = \frac{e_o^2 N_A}{4\pi\epsilon_o} \quad (10)$$

$$\lambda_{e^-,o} = e^2\left(\frac{1}{D_o} - \frac{1}{D_s}\right)\left(\frac{1}{2r_1} + \frac{1}{2r_2} - \frac{1}{r_{12}}\right) \quad (11)$$

For electron exchange between **Fe^{II}(H$_2$bim)** and **Fe^{III}-(H$_2$bim)**, the crystal structures suggest values of $r_1 = 4.9$ Å, $r_2 = 5.0$ Å, and $r_{12} = 10$ Å. Equations 8−11 then give $w_r = 2.1$ kcal mol^{-1} in MeCN and 1.7 kcal mol^{-1} in DMSO, and $\lambda_{e,o} = 17.9$ kcal mol^{-1} (MeCN) and 14.8 kcal mol^{-1} (DMSO). Although DMSO is a more polar solvent than acetonitrile, its greater optical dielectric constant allows the higher-frequency solvent modes to respond more easily to charge transfer, causing it to have the lower energy of solvent reorganization. This model predicts that $\Delta G^{\ddagger}_{e^-}$ will be 1.2 kcal mol^{-1} lower in DMSO than in MeCN, roughly consistent with the 0.8 kcal mol^{-1} difference observed. The observed positive salt effect is expected for the encounter of similarly charged species. The $\lambda_{e^-,i}$, calculated from eq 7, is 20.5 kcal mol^{-1}. Inner-sphere reorganization can in principle be calculated from bond length changes and force constants,[7] but the latter are not available for these bi-imidazoline complexes. Iron hexammine complexes should be good models for Fe(H$_2$bim)$_3^{2+/3+}$, as both involve high-spin ions and ~0.1 Å changes in Fe−N bond lengths upon electron transfer; our value of $\lambda_{e^-,i}$ is somewhat larger than the ab initio estimate of 14 kcal mol^{-1} for Fe(NH$_3$)$_6^{2+/3+}$.[46]

2. Mechanism of Hydrogen Atom Self-Exchange. The NMR experiments show that there is chemical exchange between **Fe^{II}(H$_2$bim)** and **Fe^{III}(Hbim)**, but they do not indicate the mechanism by which exchange takes place. There could be concerted movement of a proton and an electron without the presence of an intermediate. This pathway can be called proton-coupled electron transfer or hydrogen atom transfer. It is pathway *a* in Scheme 2. Alternatively, exchange could occur

(44) MeCN: $D_s = 37.5$ and $D_o = 1.7999$. DMSO: $D_s = 46.7$ and $D_o = 2.1824$ as quoted in Reimers, J. R.; Hall, L. E. *J. Am. Chem. Soc.* **1999**, *121*, 3730−3744.

(45) (a) Brown, G. M.; Sutin, N. *J. Am. Chem. Soc.* **1979**, *101*, 883−892. (b) Nielson, R. M.; Wherland, S. *J. Am. Chem. Soc.* **1985**, *107*, 1505−1510.

(46) (a) Zhou, Z.; Khan, S. U. M. *J. Phys. Chem.* **1989**, *93*, 5292−5295. (b) Calculations on Fe(tacn)$_2^{2+/3+}$: Gao, Y.-D.; Lipkowitz, K. B.; Schultz, F. A. *J. Am. Chem. Soc.* **1995**, *117*, 11932−8. (c) For a discussion on underestimation of $\lambda_{e^-,i}$ see: Formosinho, S. J.; Arnaut, L. G.; Fausto, R. *Prog. React. Kinet.* **1998**, *23*, 1−90.

Scheme 2. Possible Mechanisms for Net Hydrogen Atom Transfer

a. Hydrogen atom transfer or proton-coupled electron transfer: concerted transfer of H$^+$ and e$^-$ without the presence of an intermediate.
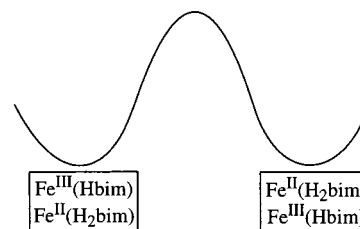
b. and *c.* Stepwise transfer of (*b*) an electron followed by a proton, or (*c*) a proton followed by an electron. These pathways involve formation of **Fe^{II}(Hbim) + Fe^{III}(H$_2$bim)** as an intermediate.

***path b*:** electron transfer followed by proton transfer

***path c*:** proton transfer followed by electron transfer
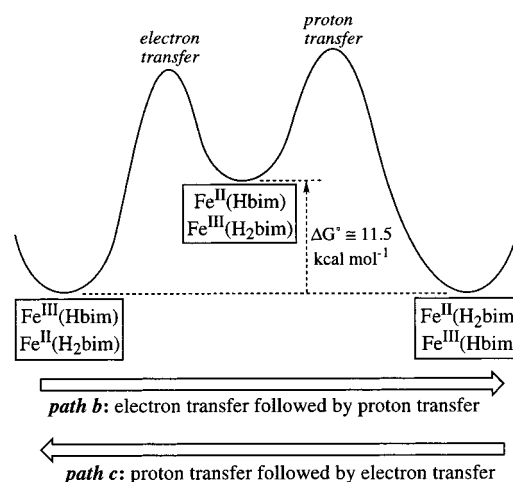
by initial electron transfer from **Fe^{II}(H$_2$bim)** to **Fe^{III}(Hbim)** to give **Fe^{II}(Hbim)** and **Fe^{III}(H$_2$bim)**, followed by proton transfer to give the products (path *b*, moving left to right at the bottom of Scheme 2). The third possibility is initial proton transfer from **Fe^{II}(H$_2$bim)** to **Fe^{III}(Hbim)**, followed by electron transfer (path *c*, right to left at the bottom of Scheme 2). Paths *b* and *c* are different, but they yield the same intermediates from the same starting materials. They are the reverse of each other, the same pathway with the arrows reversed. Therefore, by the principle of microscopic reversibility, paths *b* and *c* must occur at the same rate. They have the same $\Delta G^{\ddagger}$.

The intermediate state of paths *b* and *c*, **Fe^{III}(H$_2$bim) + Fe^{II}-(Hbim)**, is ≈11.5 kcal mol^{-1} above the ground state on the basis of the values in Scheme 1. This is almost as large as the observed barrier for net H-atom self-exchange, $\Delta G^{\ddagger}_{H^\bullet} = 12.3$ kcal mol^{-1}, which argues against a stepwise pathway. More quantitatively, Marcus theory can be used to calculate the barrier for the electron transfer step in paths *b* and *c* (eq 12; w_r from eqs 8−10). The value of ΔG° is corrected for electrostatic effects ($\Delta G^{\circ\prime} \approx 11$ kcal mol^{-1})[7e] and the intrinsic barrier (λ_{e^-}) is assumed to be the same as that determined above for **Fe^{III}-(H$_2$bim) + Fe^{II}(H$_2$bim)**, 38 kcal mol^{-1}.

$$\Delta G^{\ddagger}_{e^-} = w_r + \frac{\lambda_{e^-}}{4}\left(1 + \frac{\Delta G^{\circ\prime}}{\lambda_{e^-}}\right)^2 \quad (12)$$

The barrier to the uphill electron transfer is calculated to be 17 kcal mol^{-1}, almost 5 kcal mol^{-1} higher than the observed $\Delta G^{\ddagger}_{H^\bullet}$. The uphill electron transfer should be ca. 4000 times slower than k_{e^-}, but only a factor of 3 is observed. Thus electron

transfer is not kinetically competent to interconvert **Fe^{II}(H$_2$bim)** and **Fe^{III}(Hbim)**, ruling out paths *b* and *c*.

Therefore reaction 4 must occur by concerted transfer of an electron and a proton, effectively a neutral hydrogen atom transfer. The data do not reveal the microscopic details of this step,[2] such as the synchronicity of electron and proton movements, but they do rule out the intermediacy of **Fe^{III}(H$_2$bim)** + **Fe^{II}(Hbim)**. The 11.5 kcal mol^{-1} free energy cost to make this intermediate pair is the thermodynamic bias for one-step H-atom transfer over a stepwise path. This bias is a result of the mutual influence of the electron and proton, that **Fe^{III}-(H$_2$bim)** is a ≈0.5 V stronger oxidant than its deprotonated form **Fe^{III}(Hbim)** or (equivalently) that **Fe^{III}(H$_2$bim)** is ca. 10^8 more acidic than **Fe^{II}(H$_2$bim)**. The energetic bias in this system is apparently enough to overcome the suggested general preference for stepwise over concerted mechanisms (derived for the impact of conformational changes on long-range electron transfer).[47] The primary isotope effect $k_{NH}/k_{ND} = 2.3 \pm 0.3$ at 51 °C (324 K) is smaller than would be expected from a simple classical model of symmetrical linear hydrogen exchange.[48] Still, this is larger than the very small isotope effect $k_{OH}/k_{OD} = 1.24$ at 21 °C reported for 2,4,6-tri-*tert*-butylphenol/2,4,6-tri-*tert*-butylphenoxyl radical exchange[49] (and the small isotope effects reported for electron transfer reactions involving iron aquo and cobalt amine complexes[50]). Much larger isotope effects have been observed for Cl + HCl/DCl in the gas phase (8.6 ± 1.1 at 39.3 °C)[51] and PhCH$_2$• + PhCH$_3$/PhCD$_3$ (7.7 at 155 °C);[52] the latter is greater than the classical value of 4 at this temperature (ignoring secondary isotope effects). Quite large isotope effects have also been observed for a variety of related metal-mediated reactions. Meyer and co-workers have reported k_{OH}/k_{OD} values in the range 10−50 for a number of proton-coupled electron-transfer reactions of ruthenium−oxo complexes (some described as hydrogen atom transfers).[53] The driving force dependence of large H• transfer isotope effects has recently been discussed.[54] Isotope effects up to ~100 have been seen in a number of enzymatic reactions and model systems that involve H-atom transfer.[55] It is not clear why the very large effects are seen in some systems but not others. Perhaps the small steric demand of the bi-imidazoline ligands allows a nonlinear transition state,

(47) Hoffman, B. M.; Ratner, M. A. *J. Am. Chem. Soc.* **1987**, *109,* 6237−6243.

(48) Melander, L.; Saunders, W. H. *Reaction Rates of Isotopic Molecules*; Wiley-Interscience: New York, 1980.

(49) Arick, M. R.; Weissman, S. I. *J. Am. Chem. Soc.* **1968**, *90,* 1654.

(50) (a) Buhks, E.; Bixon, M.; Jortner, J. *J. Phys. Chem.* **1981**, *85,* 3763−3766. (b) Guarr, T.; Buhks, E.; McLendon, G. *J. Am. Chem. Soc.* **1983**, *105*, 3763−3767. (c) Friedman, H. L.; Newton, M. D. *J. Electroanal. Chem.* **1986**, *204,* 21−29.

(51) (a) Klein, F. S.; Persky, A.; Weston, R. E., Jr. *J. Chem. Phys.* **1964**, *41*, 1799−1803. (b) Garrett, B. C.; Truhlar, D. G.; Wagner, A. F.; Dunning, T. H., Jr. *J. Chem. Phys.* **1983**, *78*, 4400−4413 and references therein.

(52) Jackson, R. A.; O'Neill, D. W. *J. Chem. Soc., Chem. Commun.* **1969**, 1210−1211.

(53) (a) References 2c, 5c, 19a. (b) Binstead, R. A.; Moyer, B. A.; Samuels, G. J.; Meyer, T. J. ibid. **1981**, *103*, 2897−289. (c) Binstead, R. A.; Stultz, L. K.; Meyer, T. J. *Inorg. Chem.* **1995**, *34*, 546−551. (d) Seok, W. K.; Dobson, J. C.; Meyer, T. J. ibid. **1988**, *27,* 3−5. (e) For examples that involve H$^-$ transfer (another form of proton-coupled electron transfer), see: Roeker, L.; Meyer, T. J. *J. Am. Chem. Soc.* **1986**, *108*, 4066−4073 and ibid. **1987**, *109*, 746−754. (f) For a recent example with an osmium hydrazido complex, see Huynh, M. H. V.; Meyer, T. J.; White, P. S. *J. Am. Chem. Soc.* **1999**, *121*, 4530−1.

(54) (a) References 19b and 53f. (b) Rodkin, M. A.; Abramo, G. P.; Darula, K. E.; Ramage, D. L.; Santora, B. P.; Norton, J. R. *Organometallics* **1999**, *18,* 1106−1109. (c) Eisenberg, D. C.; Lawrie, C. J. C.; Moody, A. E.; Norton, J. R. *J. Am. Chem. Soc.* **1991**, *113*, 4888−4895.

(55) (a) Reference 2g and references therein. (b) Lewis, E. R.; Johansen, E.; Holman, T. R. ibid. **1999**, *121*, 1395−1396. (c) Mahapatra, S.; Halfen, J. A.; Tolman, W. B. *J. Am. Chem. Soc.* **1996**, *118*, 11575−11586 and references therein.

reducing k_{NH}/k_{ND} according to classical arguments,[48] and allows close approach of the complexes, which has been suggested to reduce the tunneling component.[56] Small primary kinetic isotope effects have also been reported for thermodynamically degenerate proton transfers.[57] These are believed to result when diffusion or solvent reorganization (or both) are partially rate limiting. Recent findings suggest that proton transfer may be nonadiabatic and involve extensive tunneling of H and D even when small isotope effects are observed.[58] It is possible that a similar situation obtains during H• transfer, that the reaction coordinate involves primarily low-frequency modes and the hydrogen transfer occurs by tunneling.

3. Intrinsic Barriers for Hydrogen Atom Transfer. Following eq 7, the intrinsic barrier for H-atom transfer from **Fe^{II}-(H$_2$bim)** to **Fe^{III}(Hbim)** (eq 4) is given by $\lambda_{H^\bullet} = 4(\Delta G^{\ddagger}_{H^\bullet} - w_r) = 44$ kcal mol^{-1}. The λ_o for hydrogen atom transfer reactions ($\lambda_{H^\bullet,o}$) should be very small, as this term reflects the solvent reorganization upon movement of charge, and no charge is transferred in an atom transfer process. In support of this, rate constants for hydrogen atom transfer from cyclohexane to cumyloxyl radical have been shown to be independent of solvent (<±10%) over a large range of dielectric constants, from CCl$_4$ and C$_6$H$_6$ to MeCN and MeCO$_2$H.[59] Schwarz and Endicott have similarly concluded that $\lambda_o \cong 0$ for halogen atom transfer (inner-sphere electron transfer) reactions of Co$^{II/III}$ complexes.[60] Therefore the intrinsic barrier consists primarily of inner-shell reorganization, $\lambda_{H^\bullet} \cong \lambda_{H^\bullet,i}$. This predicts that the difference in the rates of reaction in MeCN and DMSO should be predominantly due to the difference in work terms. Taking the closest contact distance ($r_{12} = 10$ Å) in the NH•••N bonded network of **Fe^{III}(Hbim)** as a model for the H-atom transfer reaction coordinate, w_r is estimated to be 1.4 kcal mol^{-1} in MeCN and 1.1 kcal mol^{-1} in DMSO. The 0.3 kcal mol^{-1} difference in calculated work terms is in reasonable agreement with the 0.7 kcal mol^{-1} difference in the observed free-energy barriers.

We suggest that $\lambda_{H^\bullet,o} \cong 0$ may prove to be a general criterion to distinguish atom transfer from other mechanistic pathways. When at least one of the reagents is uncharged, $w_r = 0$ so the condition $\lambda_{H^\bullet,o} \cong 0$ predicts that barriers will be roughly independent of solvent. This potentially provides an experimental distinction between hydrogen atom transfer and other types of proton-coupled electron transfer. For instance, large values of λ_o are anticipated for proton-coupled electron-transfer reactions in which the electron moves in one direction and the proton in another.[2] In this view, H-atom transfer is a subset of a broader class of proton-coupled electron-transfer reactions. At first glance, **Fe^{II}(H$_2$bim)** is an unlikely reagent to do hydrogen atom transfer, as the proton that is transferred is three bonds removed from the metal center that accepts the electron.

The analysis above ignores the likely formation of a hydrogen bond between **Fe^{II}(H$_2$bim)** and **Fe^{III}(Hbim)**. Bi-imidazoline complexes are capable of forming strong hydrogen bonds, as evidenced by the solid-state structure of **Fe^{III}(Hbim)** and the apparent aggregation of [**Fe^{II}(Hbim)**] in dilute solution. The **Fe^{III}(Hbim)** structure may be a good model for the precursor

(56) (a) Kreevoy, M. M.; Ostovíc, D.; Truhlar, D. G.; Garrett, B. *J. Phys. Chem.* **1986**, *90*, 3766−3774 and references therein. (b) Reference 19b.
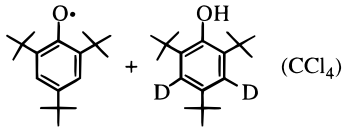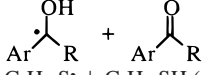
(57) Perrin, C. L.; Dwyer, T. J.; Baine, P. *J. Am. Chem. Soc.* **1994**, *116*, 4044−4049. Also see 8d and references therein.

(58) Peters, K. S.; Cashin, A.; Timbers, P. *J. Am. Chem. Soc.* **2000**, *122*, 107−113.

(59) (a) Avila, D. V.; Brown, C. E.; Ingold, K. U.; Lusztyk, J. *J. Am. Chem. Soc.* **1993**, *115*, 466−470. (b) Recent confirmation and extension: Weber, M.; Fischer, H. *J. Am. Chem. Soc.* **1999**, *121*, 7381−7388.

(60) Schwarz, C. L.; Endicott, J. F. *Inorg. Chem.* **1995**, *34*, 4572−4580 and refs. therein.

Table 4. Kinetic Data for Hydrogen Atom Self-Exchange Reactions X + H−X

X + HX	k^a	barrier^b	BDE^b	ref
H + H$_2$ (gas phase)	[8 × 10^5]	$E = 7$	104^c	65
Cl + HCl (gas phase)	[1 × 10^6]	$E = 5.5$	103^c	51
OH + H$_2$O (gas phase)	[1 × 10^5]	$E = 4.2$	119^c	66
CH$_3$• + CH$_4$ (gas phase)	[2 × 10^{-2}]^d	$E = 14$	105^c	65
t-BuO• + t-Bu$_3$COH (t-BuOOt-Bu)	∼3 × 10^4	$E = 2.6, \Delta G^{\ddagger} = 11$	105^e	67
t-BuOO• + s-BuOOH (i-C$_5$H$_{12}$)	5 × 10^2	$E = 4.5,^f \Delta G^{\ddagger} = 14$	89^e	68
(CCl$_4$) structure	2 × 10^2	$\Delta G^{\ddagger} = 14$	81^g	49
ArC(OH)R• + ArC(=O)R structure	∼4 × 10^4	$\Delta G^{\ddagger} = 13$	∼35^m	69
C$_8$H$_{17}$S• + C$_6$H$_{13}$SH (nonane)	3 × 10^4	$E = 5, \Delta G^{\ddagger} = 11$	87^h	70
C$_6$H$_5$CH$_2$• + 3-DC$_6$H$_4$CH$_3$ (toluene)	∼4 × 10^{-5}	$E = 20, \Delta G^{\ddagger} = 23$	90^i	52
Fe^{III}(Hbim) + Fe^{II}(H$_2$bim) (MeCN)	6 × 10^3	$E = 5, \Delta G^{\ddagger} = 12$	76	j
CpCr(CO)$_3$• + CpCr(CO)$_3$H (benzene)	ca. 10$^{2\,k}$	$\Delta G^{\ddagger} \cong 15$	62	18d
Tp*Mo(CO)$_3$H + Tp*Mo(CO)$_3$• (THF)^l	≤ 6 × 10^{-3}	$\Delta G^{\ddagger} \geq 20$	59^l	18c
CpW(CO)$_3$H + CpW(CO)$_3$• (benzene)	≥ 10^6	$\Delta G^{\ddagger} \leq 9$	72	18b

^{a} Rates at 298 K, in units of M^{-1} s^{-1}; gas-phase rates in square brackets. ^{b} E (Arrhenius activation energy), $\Delta G^{\ddagger}$, and H−X bond dissociation energies (BDE) in kcal mol^{-1}. ^{c} Reference 71. ^{d} Extrapolated from data for 450−800 K. ^{e} Reference 72. ^{f} Barrier for t-BuO$_2$• + 1-indanyl hydroperoxide. ^{g} Reference 73. ^{h} Bond strength for MeS−H, from ref 71. ^{i} Reference 74. ^{j} This work. ^{k} Reference 75. ^{l} Tp* = hydrotris(3,5-dimethylpyrazolyl)borate; bond strength from ref 76. ^{m} Reference 83.

complex in the H-atom transfer reaction—and for the proton self-exchange reaction (eq 3). Both the work term and the intrinsic barrier could be influenced by a hydrogen bond.[61] At this stage it is unclear how important hydrogen bond formation is to the energetics of the self-exchange reactions discussed here. Hydrogen bonding could have quite different influences on "normal" hydrogen atom abstractions by main group radicals, where the singly occupied abstracting orbital does not form hydrogen bonds,[62] versus **Fe^{III}(Hbim)** where the hydrogen-accepting orbital is essentially a nitrogen lone pair.

Early papers by Marcus, based on simple empirical bond energy−bond order calculations, suggested that activation barriers for atom transfer self-exchange reactions should be roughly 5−10% of the bond dissociation energy (BDE).[8a,63] This has been variously interpreted as the E_a $(\Delta H^{\ddagger} + RT)$[8b] or as the $\Delta G^{\ddagger}$ for self-exchange.[18b] For dissociative electron transfer e$^-$ + RX → R• + X$^-$ (a somewhat different process), Savéant's successful extension of Marcus theory gives $\Delta G^{\ddagger} = (1/4)(\text{BDE} + \lambda)$ at $\Delta G° = 0$,[9] and this has been extended to proton-transfer reactions.[10f] The barriers for reaction 4 are smaller than the prediction of the Savéant equation (>25% BDE) but fit the Marcus prediction reasonably well. The $(\Delta G^{\ddagger}_{H•} - w_r)$ of 10.9 kcal mol^{-1} is 14% of the N−H bond strength and the E_a of 4.6 kcal mol^{-1} is 6% of the bond strength. But in general, self-exchange barriers do not parallel bond strengths.[64] Kinetic data for a range of hydrogen atom self-exchange reactions (Table

4) show that the barriers do not correlate with BDEs. For instance, toluene/benzyl radical exchange is more than 10^8 slower than alcohol/alkoxyl radical exchange, even though the PhCH$_2$−H bond is 15 kcal mol^{-1} weaker than RO−H. Parameters other than the bond strength are clearly also important. A number of semiempirical approaches has been put forward to explain hydrogen atom transfer reactions A−H + B, including curve-crossing models based on singlet−triplet splittings, ionic surfaces, and antibonding between A and B.[77] The H-atom self-exchange rate constants in Table 4 follow the same trend as proton transfers, in that reactions involving O−H or N−H bonds are much faster than those involving C−H bonds. Perhaps H-atom transfer should be viewed as electron-coupled proton transfer, rather than as proton-coupled electron transfer.

(61) Kresge,[10b,c] Kreevoy (Kreevoy, M. M.; Oh, S.-W. *J. Am. Chem. Soc.* **1973**, *95*, 4805−4810), Norton,[10a,d] and others (refs 10, 29, and Robinson, B. H. in ref 10b, pp 121−152) have touched on hydrogen bonding and w_r in the context of proton transfer. Ref 62 discusses how hydrogen bonding can inhibit phenol/phenoxyl reactions.

(62) Folti, M.; Ingold, K. U.; Lusztyk, J. *J. Am. Chem. Soc.* **1994**, *116*, 9440−7.

(63) For a recent analysis of the strengths and weaknesses of the BEBO model, see Blowers, P.; Masel, R. I. *J. Phys. Chem. A* **1998**, *102*, 9957−9964.

(64) (a) See the discussion of self-exchange reactions of carbon radicals in ref 17a. (b) It should be noted that barriers for halogen atom and X$^+$ exchange often fall in the order I < Br < Cl, which is the order of M-X BDEs: (c) Schwarz, C. L.; Bullock, R. M.; Creutz, C. *J. Am Chem. Soc.* **1991**, *113*, 1225−1236 and references therein.

(65) Kerr, J. A.; Moss, S. J. *CRC Handbook of Bimolecular and Termolecular Gas Reactions*; CRC Press: Boca Raton, FL, 1981; Vol. 1, p 9 and p 187.

(66) Dubey, M. K.; Mohrschladt, R.; Donahue, N. M.; Anderson, J. G. *J. Phys. Chem. A* **1997**, *101*, 1494−1500.

(67) Griller, D.; Ingold, K. U. *J. Am. Chem. Soc.* **1974**, *96*, 630−632.

(68) Chenier, J. H. B.; Howard, J. A. *Can. J. Chem.* **1975**, *53*, 623−627.

(69) Wagner, P. J.; Zhang, Y.; Puchalski, A. E. *J. Phys. Chem.* **1993**, *97*, 13368−13374 and references therein.

(70) Alnajjar, M. S.; Garrossian, M. S.; Autrey, S. T.; Ferris, K. F.; Franz, J. A. *J. Phys. Chem.* **1992**, *96*, 7037−7043.

(71) Berkowitz, J.; Ellison, G. B.; Gutman, D. *J. Phys. Chem.* **1994**, *98*, 2744−2765.

(72) Colussi, A. J. In *Chemical Kinetics of Small Organic Radicals*; Alfassi, Z. B., Ed.; CRC Press: Boca Raton, FL, 1988; p 33.

(73) Lucanini, M.; Pedrielle, P.; Franco Pedulli, G.; Cabiddu, S.; Fattuoni, C. *J. Org. Chem.* **1996**, *61*, 9259−9263.

(74) Bierbaum, V.; DePuy, C.; Davico, G.; Eillison, B. *Int. J. Mass Spectrom. Ion Phys.* **1996**, *156*, 109−131.

(75) Reference 18d reports $k = 910$ M^{-1} s^{-1} for (C$_5$Me$_5$)Cr(CO)$_3$• + H−Cr(CO)$_2$(PPh$_3$)Cp for which $\Delta H° = -2.5$ kcal/mol, so the self-exchange rate in this system is estimated as ca. 10^2 M^{-1} s^{-1}. The rate for Cp(CO)$_3$Cr• + H−Cr(CO)$_3$Cp (mentioned in ref 18a) could be faster if steric effects are important.

(76) Skagestad, V.; Tilset, M. *J. Am. Chem. Soc.* **1993**, *115*, 5077−5083.

(77) (a) Pross, A.; Yamataka, H.; Nagase, S. *J. Phys. Org. Chem.* **1991**, *4*, 135−140 (emphasizes singlet−triplet gaps). (b) Donahue, N. M.; Clarke, J. S.; Anderson, J. G. *J. Phys. Chem. A* **1998**, *102*, 3923−3933 (emphasizes ionic states). (c) Zavitsas, A. A.; Chatgilialoglu, C. *J. Am. Chem. Soc.* **1995**, *117*, 7, 10645−10654 (emphasizes A•••B antibonding). (d) A variant and extension of the Zavitsas and Chatgilialoglu model is described in Bérces, T.; Dombi, J. *Int. J. Chem. Kinet.* **1980**, *12*, 123−139 and 183-214. (e) For an overview of the curve-crossing model, including both singlet−triplet and ionic contributions, see Shaik, S.; Shurki, A. *Angew. Chem., Int. Ed. Engl.* **1999**, *38*, 586−625. (f) Reference 64c uses a curve-crossing model with an ionic surface^b to discuss X$^+$ self-exchange between metal centers.

Table 5. Rates for Electron, Proton, and H-Atom Self-Exchange Reactions[a]

X	k_{e^-} (X + X$^-$)[a]	k_{H^+} (X$^-$ + HX)[a]	$k_{H^\bullet}$ (X + HX)[a]	ref
Fe^{III}(Hbim)	1.7×10^4 (CD$_3$CN)	$\approx 2 \times 10^6$ (CD$_3$CN)	5.8×10^3 (CD$_3$CN)	this work
CpCr(CO)$_3$$^\bullet$	unavailable	1.8×10^4 (CD$_3$CN)	ca. 10^2 (C$_6$D$_6$)[b]	79
Tp*Mo(CO)$_3$$^{\bullet c}$	8.6×10^6 (THF$-d_8$)[d]	3.5 (THF$-d_8$)[d]	$\leq 9 \times 10^{-3}$ (THF$-d_8$)[e]	18c
CpW(CO)$_3$$^\bullet$	3×10^7 (CD$_3$CN)	6.5×10^2 (CD$_3$CN)	$\geq 10^6$ (C$_6$D$_6$)	18b

[a] Rates at 298 K (unless otherwise noted), in units of M^{-1} s^{-1}. [b] Reference 75. [c] Tp* = hydrotris(3,5-dimethylpyrazolyl)borate. [d] At 303 K. [e] At 239 K.

Fe^{III}(Hbim) has previously been shown to abstract a hydrogen atom from organic molecules with weak C$-$H bonds.[6] The rate of abstraction from 9,10-dihydroanthracene roughly correlates with the rates of abstractions by *t*-BuO$^\bullet$ and *s*-BuOO$^\bullet$, following the Polanyi relation (eq 1). But only "similar" radicals fall on the same Polanyi line, and **Fe^{III}(Hbim)** and the oxygen radicals do not appear similar. This study shows that one key similarity among the three reagents is their H-atom self-exchange rates, $\log k_{H^\bullet} = 3.6 \pm 0.9$ (Table 4). Such variation is reasonable given the tightness of the Polanyi correlation.[5b,6] That the different reagents have similar self-exchange rates may prove to be a necessary condition for a Polanyi correlation.

4. Comparisons of Intrinsic Barriers for Electron, Proton, and Hydrogen Atom Transfer. All three self-exchange reactions in the iron bi-imidazoline system are quite facile ($k > 10^3$ M^{-1} s^{-1}). The intrinsic barriers, $\Delta G^{\ddagger} - w_r$, are (kcal mol^{-1}): $(1/4)\lambda_{H^+} \approx 7 < (1/4)\lambda_{e^-} = 9.6 < (1/4)\lambda_{H^\bullet} = 10.9$. It is perhaps surprising that the kinetics of electron and H-atom transfer are so similar: the rate constants differ only by a factor of 3, and the differences in $\Delta G^{\ddagger}$ and $(1/4)\lambda$ are only 0.6 and 1.3 kcal mol^{-1}. Both reactions require the inner-sphere reorganization involved in the Fe$^{III/II}$ redox couple. H-atom transfer requires, in addition, cleavage of an N$-$H bond. Presumably this is the primary contributor to $\lambda_{H^\bullet,i}$ being ca. 23 kcal mol^{-1} larger than $\lambda_{e^-,i}$. But this larger inner-sphere term is largely balanced by the absence of outer-sphere reorganization for the atom transfer. The kinetic similarity of electron and hydrogen atom transfer is apparently due to $\lambda_{e^-,o}$ being close to the additional $\lambda_{H^\bullet,i}$ associated with hydrogen movement. It should be noted that halogen atom self-exchange reactions—such as the "classical" inner-sphere reaction {CoX[L$_{N4}$](H$_2$O)}$^{2+}$ + {Co-[L$_{N4}$](H$_2$O)$_2$}$^{2+}$—can be as much as 10^6 times faster than outer-sphere electron transfer reactions of the similar compounds {Co[L][(H$_2$O)$_2$]$^{2+/3+}$}.[78]

To our knowledge, there are only three systems, X/X$^-$/X$-$H, for which the intrinsic barriers for e$^-$, H$^+$, and H$^\bullet$ transfer are all known (Table 5), the others being organometallic metal hydride complexes. The iron system is unique because of the involvement of an N$-$H bond and the separation of this bond from the redox-active metal center. The iron system is thus closer to biochemical proton-coupled electron-transfer reactions. Inspection of the kinetic data in Table 5 reveals no trend or relation between the intrinsic barriers to e$^-$, H$^+$, and H$^\bullet$ transfer. The relative rates in the iron system are $k_{H^+} > k_e > k_{H^\bullet}$, covering a range on the order of 10^2. For Tp*Mo(CO)$_3$ compounds, the range is $\geq 10^9$ and the order is $k_{e^-} > k_{H^+} \gg k_{H^\bullet}$. The CpW-(CO)$_3$ system has yet a third pattern, with k_{e^-} and $k_{H^\bullet}$ both large ($\geq 10^6$), and more than 10^3 larger than k_{H^+}. The contrast between the two metal hydride systems is remarkable, given their formal similarity. Perhaps the Tp*Mo(CO)$_3$ complexes are anomalous because of the steric demands of the Tp* ligand and its destabilization of seven-coordinate structures. The other three

systems in Table 5 show fairly close rates for electron and H-atom transfer. This is consistent with the suggestion above that the larger inner-sphere reorganization energy associated with X$-$H bond cleavage is partially offset by absence of solvent reorganization for the transfer of a neutral H$^\bullet$.

In the present work, k_{H^+} is larger than $k_{H^\bullet}$ and k_{e^-}. This contrasts with the available data on reactions of carbonylmetal-lates.[10a,d,18b,c] Proton transfer between nitrogen atoms is typically fast because little reorganization is involved, whereas significant geometrical changes occur upon deprotonation of most metal hydrides. In addition, proton transfer from **Fe^{III}(H$_2$bim)** to **Fe^{III}-(Hbim)** is likely facilitated by initial formation of a NH$\cdots$N hydrogen bond, similar to the solid state structure of **Fe^{III}-(Hbim)**. Metal hydrides and carbonylmetallates do not engage in significant hydrogen bonding.[80]

Kristjánsdóttir and Norton have shown that the proton-transfer self-exchange rates for CpM(CO)$_3$H + CpM(CO)$_3^-$ (M = Cr, Mo, W) can be used to predict rates of cross-reactions CpM-(CO)$_3$H + CpM$'$(CO)$_3^-$ using the Marcus cross-relation and assuming $f_{AB} = 1$ (eq 13).[10d] The cross-relation follows from eq 12 and the additivity postulate that the intrinsic barrier for a cross-reaction is the average of the self-exchange barriers (eq 14). Whether the additivity postulate and cross-relation will apply to hydrogen atom transfer (or proton-coupled electron transfer) and under what conditions is a topic of ongoing research. There is at least one case where eq 13 has been applied

$$k_{AB} = \sqrt{k_{AA}k_{BB}K_{AB}f_{AB}} \tag{13}$$

$$\lambda_{AB} = \frac{1}{2}(\lambda_{AA} + \lambda_{BB}) \tag{14}$$

to a proton-coupled electron-transfer reaction, the interconversion of (H$_2$O)$_5$CrOO^{2+} and (H$_2$O)$_5$CrOOH^{2+} by outer-sphere electron-transfer reagents in aqueous solution.[20] A very slow self-exchange rate of $\sim 6 \times 10^{-8}$ M^{-1} s^{-1} was derived, but it is not clear whether the proton-coupled process is described by this rate constant. Application of the Marcus cross-relation to gas-phase hydrogen atom transfer has also been discussed.[81]

Conclusions

Self-exchange rates—intrinsic barriers—have been measured for electron, hydrogen atom, and proton transfer between iron bi-imidazoline complexes. Following a Marcus theory approach, the intrinsic barrier is a direct measure of the propensity to undergo reaction in the absence of driving force. Previous studies of hydrogen atom self-exchange reactions are few, and few of these are relevant to the plethora of H-atom—or proton-coupled electron transfer—reactions of biological importance. Here the reactive sites are metal-bound ligands, potentially models for the active sites of metalloenzymes that mediate H$^\bullet$ transfer.

(78) Endicott, J.; Kumar, K.; Ramasami, T.; Rotzinger, F. P. *Prog. Inorg. Chem.* **1983**, *30*, 141. See also ref 60.

(79) Edidin, R. T.; Sullivan, J. M.; Norton, J. R. *J. Am. Chem. Soc.* **1987**, *109,* 3945$-$3953.

(80) (a) References 10a, d. (b) A rare example of an MH$\cdots$M$^-$ interaction is reported in: Brammer, L.; McCann, M. C.; Bullock, R. M.; McMullan, R. K.; Sherwood, P. *Organometallics* **1992**, *11*, 2339$-$2341.

(81) (a) References 8a$-$d, 66, and 77b and references therein.

H•, e⁻, and H⁺ self-exchange reactions of high-spin iron bi-imidazoline complexes are all facile, with (in kcal mol⁻¹ at 298 K): $\Delta G^{\ddagger}_{H^+} \approx 9 < \Delta G^{\ddagger}_{e^-} = 11.7 < \Delta G^{\ddagger}_{H^{\bullet}} = 12.3$. The fact that the redox metal is three bonds removed from the proton-accepting site does not appear to hinder net H• transfer.[82] Potentially H⁺ and H• transfer are facilitated by formation of a hydrogen bond in the precursor complex. The similarity of H-atom and electron self-exchange rate constants appears to be due to the inner-sphere reorganization component in the H-atom transfer reaction being of similar magnitude to the outer-sphere reorganization associated with the charge-transfer process.

It has previously been shown that the rate for **Fe^III(Hbim)** abstracting H• from 9,10-dihydroanthracene falls on the same Polanyi correlation (log k versus ΔH) as oxygen radicals.[6] It is proposed here that the reaction of **Fe^III(Hbim)** correlates with

reactions of oxygen radicals because these reagents have similar intrinsic barriers for H-atom abstraction. This is a new perspective on the Polanyi correlation. Further work is in progress to test these ideas, and to test the applicability of the Marcus cross-relation and additivity postulate (eqs 13, 14) to hydrogen atom transfer reactions.

Supporting Information Available: Crystallographic data for **[Fe^II(H₂bim)]**, **[Fe^III(H₂bim)]**, and **[Fe^III(Hbim)]** (PDF). This material is available free of charge via the Internet at http://pubs.acs.org.

JA9941328

(82) For a case where increasing distance between the electron-transfer and proton-transfer sites does matter, see: Baciocchi, E.; Bietti, M.; Manuchi, L.; Steenken, S. *J. Am. Chem. Soc.* **1999**, *121,* 6624−6629.

(83) Bond strength calculated from $E°$ and pK_a values in Green et al. (Green, P.; Green, W. A.; Harriman, A.; Richoux, M.-C.; Neta, P. *J. Chem. Soc., Faraday Trans. 1* **1998**, *84*, 2109) using the thermochemical cycle in Gardner et al. (Gardner, K. A.; Kuehnert, L. L.; Mayer, J. M. *Inorg. Chem.* **1997**, *36*, 2069−2078).